Flexibility of Projective-Planar Embeddings

John Maharry *
Department of Mathematics
The Ohio State University
Columbus, OH USA

Neil Robertson †
Department of Mathematics
The Ohio State University
Columbus, OH USA

Vaidy Sivaraman ‡
Department of Mathematics
The Ohio State University
Columbus, OH USA

Daniel Slilaty §
Department of Mathematics
Wright State University
Dayton, OH USA

September 26, 2011

Abstract

Given two embeddings σ_1 and σ_2 of a labeled nonplanar graph in the projective plane, we give a collection of maneuvers on projective-planar embeddings that can be used to take σ_1 to σ_2.

1 Introduction

Consider a labeled connected graph G with two cellular embeddings σ_1 and σ_2 in the projective plane. In the case that G is planar, it is shown in [8] that there are embeddings $\psi_1, \ldots, \psi_n$ of G (with $\sigma_1 = \psi_1$ and $\sigma_2 = \psi_n$) such that ψ_{i+1} is obtained from ψ_i by one of a list of given maneuvers of a graph embedded in the projective plane. In this paper we solve the same problem for the case when G is not planar. This problem has previously been considered in [10] and [18]; however, both contain errors. We will discuss these and related results (which are also mentioned in the next paragraph) in Section 6.

There are many results in the literature concerning the reembeddings of graphs in various surfaces; in particular, results relating the number of reembeddings to representativity (i.e., face width). The classical result of Whitney [20] is that any 3-connected planar graph G has a unique embedding in the plane. Robertson and Vitray [13] showed that for any orientable surface S of genus g, any 3-connected graph G embedded in Σ with representativity at least $2g + 3$ has a unique embedding in that surface. Mohar [6] and Seymour and Thomas [15] lowered this bound to $c \log(g)/\log(\log(g))$. Robertson, Zha, and Zhao [14] showed that, other than the three embeddings of $C_4 \times C_4$ in the torus, any graph with an embedding of representativity at least 4 in the torus has a unique embedding in the torus. Robertson and Mohar [7] have shown that for any surface S, there is a number $f(S)$ such that for any 3-connected

*E-mail address: maharry@math.ohio-state.edu
†E-mail address: robertso@math.ohio-state.edu
‡E-mail address: vaidy@math.ohio-state.edu
§E-mail address: daniel.slilaty@wright.edu

graph G, there are at most $f(S)$ distinct embeddings of G in S with representativity at least 3.[††] As corollaries to our main result (in Section 6) we will reprove the following three related results of Negami and Vitray for projective-planar embeddings. First, for any 3-connected graph with an embedding of representativity at least 4 in the projective plane, that is the only embedding (Theorem 6.1). Second, other than K_6, for any 5-connected graph with an embedding of representativity 3 in the projective plane, that is the only embedding (Theorem 6.2). Last, if G is 3-connected and has a 3-representative embedding in the projective plane, then the number of embeddings of G in the projective plane is a divisor of 12 (Theorem 6.3).

Before we state our main result, we would also like to mention a relationship between this problem and a problem on signed graphs. If Σ_1 and Σ_2 are two signed graphs with the same labeled edge set, then when does $M(\Sigma_1) = M(\Sigma_2)$? (Here $M(\Sigma_i)$ is the frame matroid of the signed graph Σ_i. See [21] for an introduction to signed graphs and their matroids.) Since the relationship between different representations of the same matroid is very important in matroid theory, an answer to this question is desirable. In [16] it is shown that if $M(\Sigma_1)$ is connected and not graphic, then $M(\Sigma_1) = M^*(G)$ for some ordinary graph G iff Σ_1 and G are topological duals in the projective plane. So if $M(\Sigma_1) = M(\Sigma_2) = M^*(G)$ is 3-connected, then Whitney's 2-Isomorphism Theorem (see, for example, [11, Sec.5.3]) tells us that G is the only ordinary graph that represents $M^*(G)$. Thus the difference between Σ_1 and Σ_2 is just that they are duals of two distinct embeddings of G in the projective plane. Hence this problem of signed-graph matroid isomorphism contains the reembedding problem of projective-planar graphs as a special case.

In Section 2, we will define three operations on a graph embedded in the projective plane: Q-Twists, P-Twists, and W-Twists. (Here Q, P, and W stand for quadrilateral, Petersen, and Whitney.) Our result is the following.

Theorem 1.1. *Let G be a connected, nonplanar graph. If σ_1 and σ_2 are two embeddings of G on the projective plane, then there exists a sequence of Q-Twists, P-Twists, and W-Twists taking σ_1 to σ_2.*

Our main lemma to the proof of Theorem 1.1 (which we spend the vast majority of the paper proving) is Lemma 1.2.

Lemma 1.2. *Let G be a 3-connected, nonplanar graph. If σ_1 and σ_2 are two embeddings of G on the projective plane, then there exists a sequence of Q-Twists and P-Twists taking σ_1 to σ_2.*

A natural approach to proving Lemma 1.2 would be to find a topological subgraph H of G with known flexibility in the projective plane and then examine the H-bridges and how they behave under the flexibility of H. A natural candidate for H would be $K_{3,3}$-subdivision because G is guaranteed to have it unless $G \cong K_5$. However, it seems to us that such an approach is not feasible and so we start with a subgraph H that is a subdivision of the Wagner graph V_8. The Wagner graph V_8 (also called the 4-rung Möbius Ladder) is obtained from an 8-cycle on vertices $v_1, v_2, \ldots, v_8$ by adding four $v_i v_{i+4}$-chords. In any projective-planar embedding of V_8 its octagon must be embedded contractibly; with $K_{3,3}$ there is no such cycle that is guaranteed to be contractible. This property of V_8 makes a proof of Lemma 1.2 starting with a V_8-subdivision tractable as the reader will see in Section 4. Thus we split the proof of Lemma 1.2 into two cases: where G contains a V_8-minor (Section 4) and where G is V_8-free (Section 5). The V_8-free case is facilitated by Theorem 1.3 which is a result proven independently by both Kelmans and Robertson but remains unpublished. One might ask whether one could extend the techniques of Section 4 to graphs with a $K_{3,3}$-minor but no V_8-minor in order to avoid using Theorem 1.3. We contend that such an approach would actually just reproduce much of the details of a proof of Theorem 1.3.

[††]They also give examples to show that no such bound exists depending only on the surface for highly-connected 2-representative embeddings.

Theorem 1.3. *Let G be an internally 4-connected graph with no V_8-minor. Then G belongs to one of the following families:*

1. *Planar graphs*
2. *Subgraphs of double wheels (i.e., there exist two vertices a, b of G such that $G \setminus \{a, b\}$ is a cycle)*
3. *Graphs with a 4-vertex edge cover (i.e., there exist four vertices a, b, c, d of G such that $V(G) \setminus \{a, b, c, d\}$ is edgeless)*
4. *The line graph of $K_{3,3}$*
5. *Graphs with seven or fewer vertices*

2 Twisting Operations

A *Q-Twist* is one of the operations described in this paragraph. The *full* Q-Twist operation *hinged* at $1, 2, 3, 4$ and *latched* at A, B is the operation shown in Figure 1 for a graph embedded in the projective plane. One can identify and/or delete hinges and latches of the full Q-Twist to obtain a *degenerate* Q-Twist. Several degenerate Q-Twists are shown in Figure 2. For the rightmost degenerate Q-Twist, when the light grey block is a single edge we often refer to this operation as *flipping* an edge.

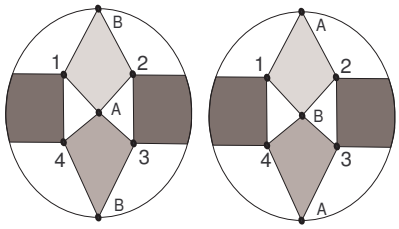

Figure 1.
The Q-Twist operation hinged at $1, 2, 3, 4$ and latched at A, B.

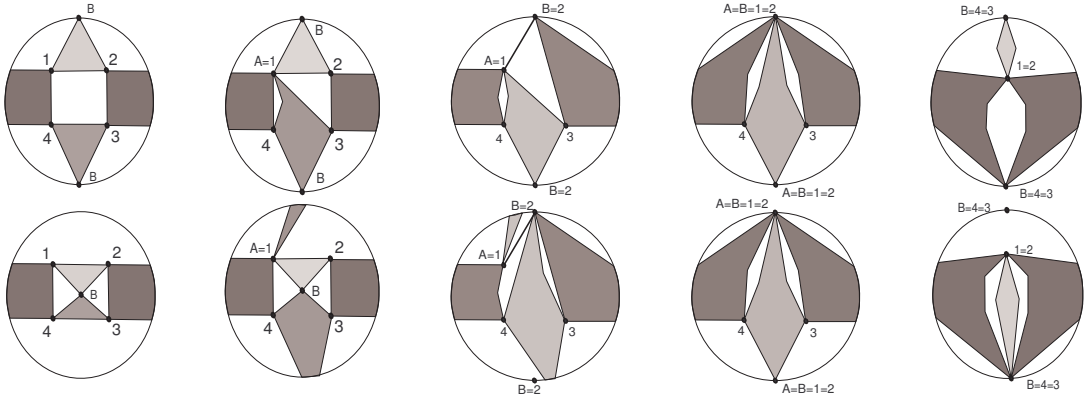

Figure 2.

A *P-Twist* is one of the operations described in this paragraph. The *full* P-Twist is the operation shown in the first column of Figure 3 for a graph embedded in the projective plane. The second and third columns of Figure 3 are different drawings of the P-Twist. We refer these three drawings, respectively, as the 'bowtie', 'central', and 'pentagonal' views. A *degenerate* P-Twist is obtained from a full P-Twist by contracting a triangular patch or by contracting one side of a triangular patch. In Figure 4 we show three typical degenerate P-Twists all obtained from the bowtie view of the full P-Twist. The first is

obtained by contracting patches 2,4,8,9, the second is obtained by contracting patch 5, and the third is obtained from the second by contracting the dark patches to two edges as labeled

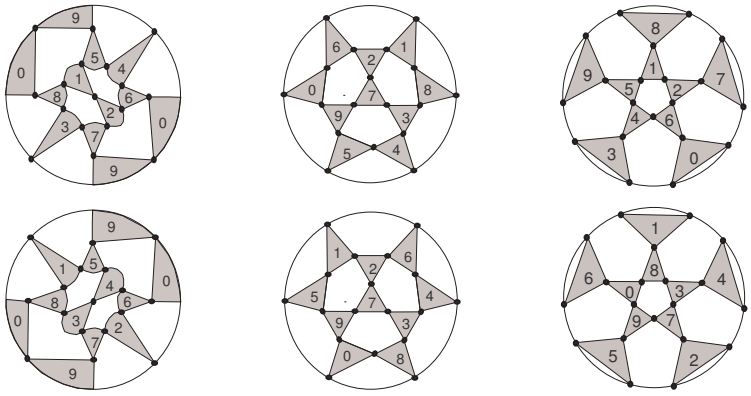

Figure 3.

The three views of the P-Twist

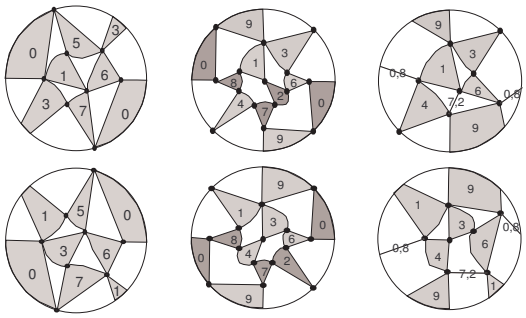

Figure 4.

It is worth noting that the full P-Twist without the shading in the triangles is the line graph of the Petersen graph, call it $L(P)$ where P is the Petersen graph. One can check that there are exactly two distinct embeddings of P. Now since P is cubic, each embedding of P extends uniquely to an embedding of $L(P)$ and any embedding of $L(P)$ comes from an embedding of P. Hence there are only two embeddings of $L(P)$ and these embeddings are related by the full P-Twist. Furthermore, the two embeddings cannot be related by a Q-Twist (or a sequence of Q-Twists) because in a Q-Twist there are at most 6 vertices whose rotation of edges (up to reversal) is changed by the operation. In the two embeddings of the line graph of the Petersen graph this change in rotation occurs at all 15 vertices.

Finally, a *W-Twist* hinged on vertices A and B is the operation shown in Figure 5.

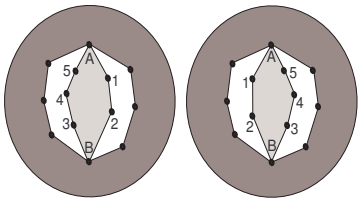

Figure 5.

3 Proof of Theorem 1.1

In this section we prove Theorem 1.1 assuming Lemma 1.2. Our proof will proceed by induction on $|V(G)| + |E(G)|$. In the base case $|V(G)| + |E(G)| = 15$ and so $G \cong K_5$ or $K_{3,3}$ which are both 3-connected. The result then follows by Lemma 1.2. Suppose now that $|V(G)| + |E(G)| > 15$ and G is connected but not 3-connected (the 3-connected case follows by Lemma 1.2).

Proposition 3.1. *If G is connected, nonplanar, projective planar, and not 3-connected, then $G = H \oplus_t P$ for $t \in \{1, 2\}$ where P is planar and H is not.*

Proof. Given that G is connected but not 3-connected, $G = H \oplus_t P$ for $t \in \{1, 2\}$. Since planarity is closed under 1-sums and 2-sums, then without loss of generality H is not planar. It must be that P is planar because otherwise G will contain one of the twelve excluded minors for projective planarity that are not 3-connected. A proof for $t = 1$ is evident and a proof for $t = 2$ can be found in [12, §3]. □

Hence we can assume that $G = H \oplus_t P$ for $t \in \{1, 2\}$ where P is planar and H is not. Let $\{x, y\}$ be the vertices of the separation and e be the xy-edge of H and P. So if σ_1 and σ_2 are distinct embeddings of G in the projective plane, these restrict to embeddings $\sigma_i|_H$ and $\sigma_i|_P$ where the embeddings of P are planar embeddings inside a disk. Hence, by induction, there is a sequence of Q-, P- and W-twists that takes $\sigma_1|_H$ to $\sigma_2|_H$. Also by Whitney's theorem [9, Thm 2.6.8], there is a sequence of W-twists that takes $\sigma_1|_P$ to $\sigma_2|_P$. These operations on H and on P can all be performed independently of each other.

4 Proof of Lemma 1.2 for graphs with a V_8-minor

The *n-rung Möbius ladder* V_{2n} is the graph obtained from the cycle on vertex set $\{1, 2, \ldots, 2n\}$ by adding an $(i, n+i)$-edge for each $1 \leq i \leq n$. Note that $V_4 \cong K_4$ and $V_6 \cong K_{3,3}$. In this section we prove Lemma 1.2 in the case that G has a V_{2n}-minor for some $n \geq 4$.

Let ν_0 be the canonical projective-planar embedding of V_{2n} with a facial $2n$-cycle. Let ν_i with $i \in \{1, 2, \ldots, n\}$ be the embedding obtained from ν_0 by flipping in the $(i, i+n)$-chord. (Figure 6 shows the embeddings ν_0 and ν_4 for V_8.) For $n \geq 4$, one can check that there is no embedding of V_{2n} in which the $2n$-cycle is noncontractible. Hence $\nu_0, \nu_1, \ldots, \nu_n$ are all of the embeddings of V_{2n} for $n \geq 4$.

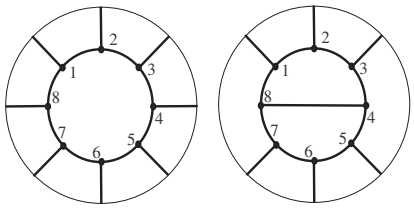

Figure 6.

Now let G be a 3-connected graph with two distinct embeddings on the projective plane, σ_1 and σ_2. Let H be a V_{2n}-subdivision contained in G with n a maximum. Since G is 3-connected we can now rechoose H so that it has no local H-bridges (see, e.g., [3, Lemma 6.2.1]). This implies that any branch of H that can be chosen to be a single edge is chosen as such. Let $\gamma_{i,j}$ be the branch of H corresponding to the (i, j)-edge of V_{2n} and let C_H be the cycle in H corresponding to the $2n$-cycle of V_{2n}.

Let $\sigma_1|_H$ and $\sigma_2|_H$ be the restrictions of the two embeddings σ_1 and σ_2 to H. Without loss of generality, we can split the problem into the following five cases. In Case 1, suppose $\sigma_1|_H = \sigma_2|_H = \nu_0$. In Case 2, suppose $\sigma_1|_H = \nu_0$ and $\sigma_2|_H = \nu_1$. In Case 3, suppose $\sigma_1|_H = \sigma_2|_H = \nu_1$. In Case 4, suppose $\sigma_1|_H = \nu_1$ and $\sigma_2|_H = \nu_2$. Finally, in Case 5, suppose $\sigma_1|_H = \nu_1$ and $\sigma_2|_H = \nu_k$ with $k \in \{3, n-1\}$.

Before beginning our case analysis, we will describe some general principles that we will use in all (or most) of the cases.

Two embeddings of G in a closed surface S are the same iff they have the same facial boundary walks iff G is fixed pointwise up to isotopy on S. Consider any embedding ψ of G in the projective plane. Since any embedding of $H \subseteq G$ is 2-representative, every facial boundary of H is a cycle in G. Now let A be a facial boundary cycle of H of length ℓ, let $B_1, \ldots, B_t$ be the H-bridges of G that are embedded inside of A, and let K be the graph $K_{1,\ell}$ with degree-1 vertices to be attached to the vertices of A. Since G is 3-connected, we get that $K \cup A \cup B_1 \cup \cdots \cup B_t$ is a 3-connected planar graph. As such the facial

cycles of $K \cup A \cup B_1 \cup \cdots \cup B_t$ are uniquely determined. Thus an embedding ψ of G in the projective plane is uniquely determined by which face of H a given bridge is embedded in.

Since C_H is contractible in all embeddings of H, we say that an H-bridge B is *reembedded* with respect to σ_1 and σ_2 if B is inside the disk region of C_H in exactly one of the embeddings. Otherwise, we say B is *fixed* with respect to σ_1 and σ_2. We call B *reembeddable* when there is an embedding σ_2' of $H \cup B$ with $\sigma_2'|_H = \sigma_2|_H$ such that B is reembedded with respect to σ_1 and σ_2'. Evidently any reembedded bridge is reembeddable and a fixed bridge may or may not be reembeddable.

Given σ_1 and σ_2, let $\overline{H}$ be the subgraph of H with edges and interior vertices of the chords of C_H that are flipped relative to σ_1 and σ_2 removed. We call this the *fixed subgraph* of H. Note that in Cases 1 and 3, $\overline{H} = H$; in Case 2, $\overline{H}$ is a V_{2n-2}-subdivision with $2n-2 \geq 6$; and in Cases 4 and 5, $\overline{H}$ is a V_{2n-4}-subdivision with $2n-4 \geq 4$. In Case 3, $\sigma_1|_{\overline{H}} = \sigma_2|_{\overline{H}} = \nu_1$ and in all the remaining cases, $\sigma_1|_{\overline{H}} = \sigma_2|_{\overline{H}} = \nu_0$. So now in Cases 1–3 (because $2n-2 \geq 6$) the face of $\overline{H}$ in which a given H-bridge B is embedded in σ_k is uniquely determined by whether B is interior or exterior to C_H in σ_k. Thus the embeddings σ_1 and σ_2 when restricted to $\overline{H} \cup B$ are the same (i.e., fixed pointwise up to isotopy) iff B is a fixed bridge. In Cases 4 and 5 with $n \geq 5$, we get the same result for H-bridges and $\overline{H}$. In Case 4 with $n = 4$, we do not, a priori, get this result for the faces of B in $\overline{H}$. The only time this might fail is when B has all of its attachments are on the $\gamma_{3,7}$- and $\gamma_{4,8}$-chords because there are exactly two faces in $\overline{H}$ that are exterior to C_H and B may be embedded in either one. In this case, however, since one of the faces of $\overline{H}$ exterior to C_H is also a face of H, this cannot happen. So again in Case 4 we get that σ_1 and σ_2 restricted to $\overline{H} \cup B$ are the same iff B is a fixed bridge. In Case 5 with $n = 4$, this possibility does indeed happen (e.g., with the two embeddings of the Petersen graph relative to any V_8-subdivision). Therefore in all cases save Case 5 with $n = 4$, the embeddings σ_1 and σ_2 restricted to $\overline{H}$ and its fixed H-bridges are the same embeddings. That is the difference between σ_1 and σ_2 is described exactly by which H-bridges are reembedded. In Case 5 with $n = 4$, we do not use the terms fixed and reembedded.

Two H-bridges in G with attachments on a cycle C are called *skewed* with respect to C if they share three common attachments on C or have pairs of alternating attachments on C. Also we say that B *belongs* to face F of H in ν_i if all of its attachments are on F. Note that if two H-bridges B_1 and B_2 both belong to F and are skewed with respect to F then one of B_1 and B_2 must belong to some other face as well.

The basic strategy for each case (except Case 5 with $n = 4$) is to first identify what the reembeddable H-bridges are and then to define a sequence of Q-Twists taking σ_1 to σ_2. In this proof for graphs with V_8-minors, P-Twists only appear in Case 5 with $n = 4$. When defining a potential twist we must always verify that there are no bridges (fixed or otherwise) that obstruct it.

Case 1: Note that any H-bridge B is reembeddable iff all of the attachments of B are on $\gamma_{i,i+1} \cup \gamma_{i+n,i+1+n}$ for some $i \in \{1, 2, \ldots, n\}$. So then each reembeddable bridge belongs to C_H and the other face of $\sigma_1|_H = \sigma_2|_H$ with $\gamma_{i,i+1} \cup \gamma_{i+n,i+n+1}$ on its boundary. Call this latter face F_i.

If B is reembeddable, then either B is a single edge with one endpoint on $\gamma_{i,i+1}$ and the other on $\gamma_{n+i,n+i+1}$, B has exactly one attachment on either $\gamma_{i,i+1}$ or $\gamma_{i+n,i+n+1}$ and at least two attachments on the other as on the left in Figure 7, or B has a cut-vertex in its interior as on the right in Figure 7. We will call single-edge bridges I-type bridges, the second kind V-type bridges, and the last kind X-type bridges. For V-type bridges, let the singular attachment be called its *apex*.

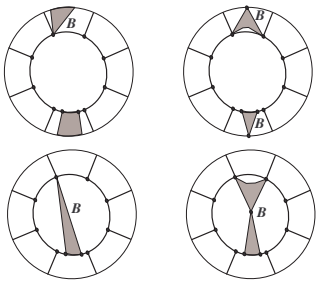

Figure 7.

As V_{2n} was taken with n maximal, we get the following restrictions on these three reembeddable types of bridges. For I-type bridges, at least one attachment must be a branch vertex of H. For V-type bridges, either the apex is a branch vertex of H or all of the non-apex attachments are branch vertices of H. These will be called V_{end}-type and V_{int}-type for apex on a branch vertex and apex in the interior of a branch, respectively. For X-type bridges, they cannot have interior attachments on both branches.

If $B_1, \ldots, B_k$ are all reembeddable, all non-skewed with respect to C_H, and all interior to C_H in σ_j then $B_1, \ldots, B_k$ all must belong to the same F_i. The restrictions on the bridge structures in the previous paragraph yield the following possible configurations for $\gamma_{i,i+1} \cup \gamma_{i+n,i+n+1} \cup B_1 \cup \cdots \cup B_k$ inside C_H. If there is a V_{int}-type bridge in $\{B_1, \ldots, B_k\}$, then the remaining bridges in $\{B_1, \ldots, B_k\}$ must all be V_{end}-type and I-type and $\gamma_{i,i+1} \cup \gamma_{i+n,i+n+1} \cup B_1 \cup \cdots \cup B_k$ must be as on the left of Figure 8. If there is an X-type bridge in $\{B_1, \ldots, B_k\}$, then the remaining bridges in $\{B_1, \ldots, B_k\}$ must all be V_{end}-type and I-type and $\gamma_{i,i+1} \cup \gamma_{i+n,i+n+1} \cup B_1 \cup \cdots \cup B_k$ must be as in the second configuration in Figure 8. If there is no V_{int}-type or X-type bridge in $\{B_1, \ldots, B_k\}$, then $\gamma_{i,i+1} \cup \gamma_{i+n,i+n+1} \cup B_1 \cup \cdots \cup B_k$ have one of the two remaining types of configurations in Figure 8.

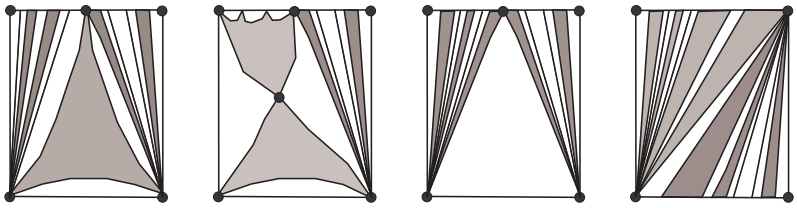

Figure 8.
Configurations of reembeddable non-skewed bridges interior to C_H

A collection $\mathcal{F}$ of reembeddable V-type and I-type bridges sharing the same apex a and embedded in the same face of H is called a *fan* with apex a. The other attachments of the bridges in $\mathcal{F}$ must all lie on the same branch of H. We will call the first and last such attachments on this branch the *extreme feet of* $\mathcal{F}$. So now if $\mathcal{B}' \subseteq \{B_1, \ldots, B_k\}$ are bridges that are reembedded from σ_1 to σ_2, since there cannot be disjoint H-paths from $\gamma_{i,i+1}$ to $\gamma_{i+n,i+n+1}$ within the bridges of $\mathcal{B}'$, either $\mathcal{B}'$ is a single X-type bridge or a fan. As with V-type bridges, we further describe fans as *interior* fans or *endpoint* fans for when the apex is in the interior of a branch of H or on a branch vertex of H. Interior fans consist of at most one V_{int}-type bridge along with at most two I-type bridges. We do not consider a single I-type bridge as an interior fan.

Since $\sigma_1 \neq \sigma_2$, there is some reembedded H-bridge. Either all of the reembedded bridges belong to some F_i or not. Let the latter possibility be Case 1.1 and the former possibility be Case 1.2.

Case 1.1 Since reembeddable bridges belonging to different F_i's are skewed with respect to C_H, each reembedded bridge belongs to one of F_i and F_j for some $i \neq j$. Let $\mathcal{B}_i$ be the collection of reembeddable bridges belonging to F_i and $\mathcal{B}_j$ be the collection of reembeddable bridges belonging to F_j. Let $\mathcal{B}'_i \subseteq \mathcal{B}_i$ and $\mathcal{B}'_j \subseteq \mathcal{B}_j$ be the bridges that are actually reembedded. Since bridges in $\mathcal{B}_i$ are skewed on C_H to bridges in $\mathcal{B}_j$, we have without loss of generality, that the bridges of $\mathcal{B}'_i$ are interior to C_H in σ_1, the

bridges of $\mathcal{B}'_j$ are interior to C_H in σ_2, and the bridges of $\mathcal{B}_i \setminus \mathcal{B}'_i$ and $\mathcal{B}_j \setminus \mathcal{B}'_j$ are all exterior to C_H. We can now go from σ_1 to σ_2 by first reembedding each bridge of $\mathcal{B}'_i$ individually by a degenerate Q-Twist. (We cannot necessarily reembed $\mathcal{B}'_i$ all at once when it is a fan as there may be reembeddable but fixed bridges that block this.) We then reembed each bridge of $\mathcal{B}'_j$ individually by a single degenerate Q-Twist.

Case 1.2 Let $\mathcal{B}$ be the reembbedable bridges belonging to F_i and $\mathcal{B}' \subseteq \mathcal{B}$ be the ones that are actually reembedded. In Case 1.2.1 there is an X-type bridge in $\mathcal{B}'$. In Case 1.2.2 say there is no X-type bridge in $\mathcal{B}'$ and there an interior fan in $\mathcal{B}'$. In Case 1.2.3 say there is no X-type and no interior fan in $\mathcal{B}'$.

Case 1.2.1 If there is an X-type bridge $X \in \mathcal{B}'$, then say without loss of generality X is interior to C_H in σ_1. Thus the remaining bridges in $\mathcal{B}'$ are all exterior to C_H in σ_1. Hence $\mathcal{B}' \setminus X$ is either a single X-type bridge or $\mathcal{B}' \setminus X$ is a fan with apex a. If $\mathcal{B}' \setminus X$ is a single X-type bridge, call it X', then we go from σ_1 to σ_2 by one full Q-Twist hinged on the extreme attachments of $X \cup X'$ on $\gamma_{i,i+1}$ and $\gamma_{i+n,i+n+1}$ and latched at the cut vertices in the interiors of X and X'. If $\mathcal{B}' \setminus X$ is a fan with apex a, then we go from σ_1 to σ_2 by one Q-Twist hinged on the extreme attachments of $\mathcal{B}'$ on $\gamma_{i,i+1}$ and $\gamma_{i+n,i+n+1}$ and latched at the cut vertex in the interior of X and at a save in embeddings like the one on the left in Figure 9 where there are bridges in the fan $\mathcal{B}' \setminus X$ whose non-apex attachments are on a path not intersecting the paths between the extreme feet of X. Each of these bridges must first be reembedded individually by degenerate Q-Twists to obtain embedding σ'_1 shown on the far right of Figure 9. Let $\mathcal{B}'' \subseteq \mathcal{B}'$ be the bridges remaining in F_i in σ'_1. We now go from σ'_1 to σ_2 (the second embedding in Figure 9) by a Q-Twist hinged on the extreme feet of $\mathcal{B}'' \cup X$ and latched on a and the cut vertex of X.

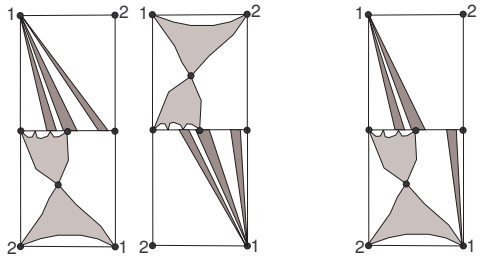

Figure 9. Case 1.2.1: The lower quadrilateral is the interior of C_H.

Case 1.2.2 Let V be the reembedded interior fan. Without loss of generality, assume that V is interior to C_H in σ_1. If $\mathcal{B}' = V$, then we can go from σ_1 to σ_2 by a single degenerate Q-Twist. Otherwise, $\mathcal{B}' \setminus V$ is an interior or end fan inside F_i in σ_1. Let these be Cases 1.2.2.1 and 1.2.2.2.

Case 1.2.2.1 If there is also an interior fan, call it N, in $\mathcal{B}' \setminus V$, then the possibilities for $\mathcal{B}'$ in σ_1 are shown in the first three configurations of Figure 10. We show the configurations with V_{int} bridges included, but they actually need not be there or need not be reembedded; however they can be added and/or made reembeded as there can be no other types of H-bridges blocking this modification. We can now go from σ_1 to σ_2 by a single Q-Twist hinged on the extreme attachments of V and N when there is no fixed V_{int}-type bridge in V or N; otherwise, we go from σ_1 to σ_2 by two such Q-Twists where the first Q-Twist reembeds the V_{int}-type bridge(s) in V and N and the second puts them back.

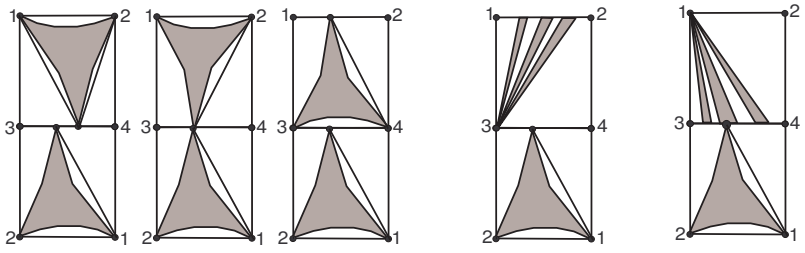

Figure 10. Case 1.2.2: The lower quadrilateral is the interior of C_H.

Case 1.2.2.2 Let $N = \mathcal{B}' \setminus V$. The apex of N is either on the same branch of H as the apex of V or not. In the latter case, the configuration for V and N is the fourth one shown in Figure 10. (Again the V_{int}-type bridge might not be in V, but can be added to it.) We can now go from σ_1 to σ_2 by a single Q-Twists hinged on the non-apex attachments of V and latched at the apices of V and N. No fixed bridges can block this.

In the former case, the configuration for V and N is last shown in Figure 10. Let N_r be the bridges of N whose extreme attachments are both at or to the right of the apex of V. We now go from σ_1 to σ_2 by first performing Q-Twists to individually reembed each bridge in N_r. Second, for the remaining bridges of $N \setminus N_r$, there can be no fixed H-bridges with attachments on the path connecting the extreme attachments of $N \setminus N_r$. Hence we can now perform a Q-Twist hinged on the extreme attachments of $N \setminus N_r$ and V and latched on the apex vertices of N and V.

Case 1.2.3 Here $\mathcal{B}'$ consists of one or two end fans. We assume that there are two as the details for just one are contained in the proof for two. Denote these two fans by N_1 and N_2. We split this Case into the following subcases: in Case 1.2.3.1, both fans share the same apex, say a on $\gamma_{i,i+1}$; in Case 1.2.3.2, the apices of the fans are the distinct endpoints of $\gamma_{i,i+1}$; in Case 1.2.3.3, the apices of the two fans are on different branches.

Case 1.2.3.1 The fan N_j is contained in a possibly larger fan $\overline{N}_j$ with apex a which might include reembedable but fixed bridges. Such bridges are shown in black in Figure 11. Consider two H-bridges $B_1 \in \overline{N}_1$ and $B_2 \in \overline{N}_2$ whose paths between their extreme feet on $\gamma_{i+n,i+1+n}$ overlap in at least an edge. It must be that B_1 and B_2 are both fixed or both reembedded. Therefore, the path $\gamma_{i+n,i+1+n}$ decomposes into subpaths $P_1, \ldots, P_k$ (some possibly of length zero) with the following properties: first, $P_m \cap P_{m+1}$ is a single vertex for each $1 \leq m \leq k-1$; second, each bridge in $\overline{N}_1 \cup \overline{N}_2$ has all of its attachments (aside from a) on some in P_l; third, each I-type bridge in $\overline{N}_1 \cup \overline{N}_2$ can then be assigned to a single P_l containing its non-apex attachment such that all of the bridges which are assigned to P_l are either all reembedded or all fixed; and fourth, if all bridges assigned to P_l are fixed, then all bridges assigned to P_{l+1} are all reembedded. Thus we can take σ_1 to σ_2 by a sequence of $\lceil \frac{k}{2} \rceil$ degenerate Q-twists, hinged at endpoints of the P_l's and latched at a.

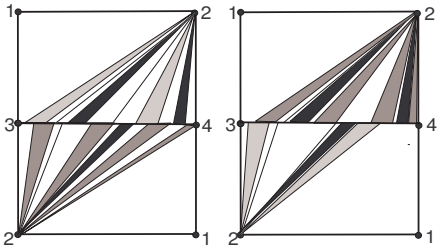

Figure 11.
Case 1.2.3.1: Fixed bridges are shown in black.

Case 1.2.3.2 Let a_t be the apex of N_t. Without loss of generality, say N_1 is interior to C_H in σ_1. The first embedding in Figure 12 shows N_1 and N_2 in σ_1 where the lower quadrilateral is interior to C_H. The second embedding in Figure 12 shows N_1 and N_2 in σ_2. Given $\{j,k\} = \{1,2\}$, it may be the case that there are bridges in N_j that have no attachment on $\gamma_{i+n,i+1+n}$ that is to the left of the rightmost attachment of N_k. If so, then assume without loss of generality that $j = 1$ such as what is shown in Figure 12. Let $N_1' \subseteq N_1$ be the collection of these bridges. Each individual bridge in N_1' may be reembedded using a degenerate Q-Twist to obtain embedding σ_1' shown as the third embedding in Figure 12. Now given $\{x,y\} = \{1,2\}$, it may be the case that there are bridges in N_x that have no attachment on $\gamma_{i+n,i+1+n}$ that is to the right of the leftmost attachment of N_y. We reembed all of the bridges in $N_2 \cup (N_1 \setminus N_1')$ save these by a single Q-Twist (no fixed bridge may block this Q-Twist) to obtain embedding σ_2' such as what is shown as the fourth embedding of Figure 12. Finally we go from σ_2' to σ_2 by performing individual Q-Twists on each of the remaining bridges of $\mathcal{B}'$.

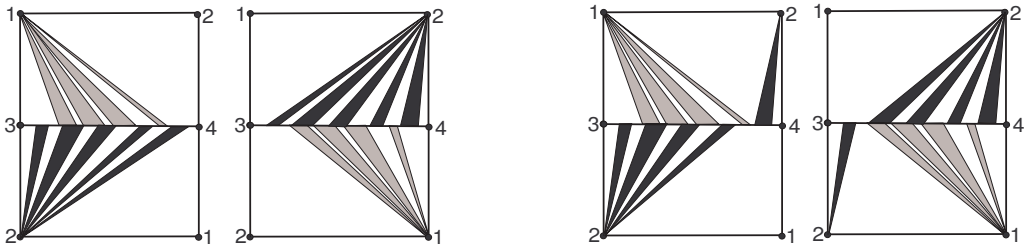

Figure 12.

Case 1.2.3.2

Case 1.2.3.3 Let a_t be the apex of N_t. Because a_1 and a_2 are on different branches of H, the bridges of N_1 are skewed to the bridges of N_2 in one of F_i or C_H and not in the other. Without loss of generality, say N_1 is embedded in the skewed face in σ_1. In Figure 13 the skewed face is the lower square region, the first and second embeddings are σ_1 and σ_2. We may now reembed each bridge of N_1 individually by a Q-Twist to obtain the the third embedding in Figure 13. We then reembed each bridge of N_2 individually by a Q-Twist to obtain σ_2.

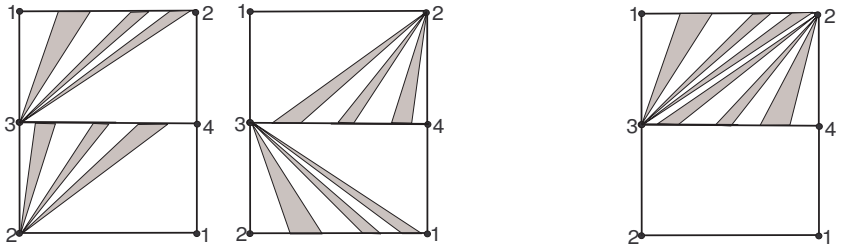

Figure 13.

Case 1.2.3.3

Case 2 Suppose $\sigma_1|_H = \nu_0$ and $\sigma_2|_H = \nu_1$ (See Figure 14).

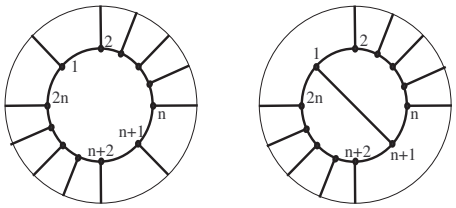

Figure 14.

Embeddings of H in Case 2

There are three types of H-bridges that are reembeddable. First, any H-bridge B with attachments in the interior of $\gamma_{1,n+1}$ must be reembedded and so all of the other attachments of B are on exactly one of $\gamma_{1,2}$, $\gamma_{1,2n}$, $\gamma_{n,n+1}$, $\gamma_{n+1,n+2}$. Let B_2, B_{2n}, B_n, and B_{n+2}, respectively, be the collections of these bridges with attachments on the interior $\gamma_{1,n+1}$. Second, H-bridges that have all attachments on $\gamma_{2n,1} \cup \gamma_{1,2}$ or all attachments on $\gamma_{n,n+1} \cup \gamma_{n+1,n+2}$. These types of bridges must be reembedded and we denote the collections of these bridges by B_1 and B_{n+1}. Let $\mathcal{B}$ be the collection of all of these bridges in B_z along with $\gamma_{1,n+1}$. Third, bridges with attachments on both paths $\gamma_{2n,1} \cup \gamma_{1,2}$ and $\gamma_{n,n+1} \cup \gamma_{n+1,n+2}$. Let $\mathcal{A}$ denote the collection of these types of bridges.

Recall that for any collection of reembedded H-bridges that are all interior or all exterior to C_H, there must be a vertex c which prevents two vertex-disjoint C_H-paths in the collection because any two such paths would cross if reembedded.

Let α_1 be the subpath of $\gamma_{2n,1} \cup \gamma_{1,2}$ between the extreme attachments of $\mathcal{B}$. Let β_1 be the similarly defined subpath of $\gamma_{n+2,n+1} \cup \gamma_{n+1,n}$. Any H-bridge in $\mathcal{A}$ exterior to C_H in σ_2 with attachments producing

an H-path that would cross some H-path of $\mathcal{B}$ if it were drawn exterior to C_H must be a reembedded bridge. Let $\mathcal{A}_1$ be the collection of such H-bridges. Now let $H_1 = H \cup (\bigcup \mathcal{B})^{\dagger\dagger}$ and we can perform a Q-twist hinged on the endpoints of α_1 and β_1 in $\sigma_2|_{H_1}$ and latched at some vertex $c_1 \in \gamma_{1,n+1}$. If this Q-Twist can be extended to all of G in σ_2, then we obtain an embedding σ_3 for which $\sigma_1|_H = \sigma_3|_H = \nu_0$ and then we can go from σ_1 to σ_3 by a sequence of Q-Twists as in Case 1. If we cannot perform this Q-Twist on all of G, then $\mathcal{A}_1 \neq \emptyset$. Let $H_2 = H_1 \cup (\bigcup \mathcal{A}_1)$, α_2 extends α_1 to the extreme attachments of $\mathcal{A}_1$ on $\gamma_{2n,1} \cup \gamma_{1,2}$, and β_2 extends β_1 similarly. Any H-bridge interior to C_H in σ_2 with attachments producing an H-path that would cross some H-path of $\bigcup(\mathcal{B} \cup \mathcal{A}_1)$ if it were drawn interior to C_H must be a reembedded bridge. Let $\mathcal{A}_2$ be the collection of such H-bridges. We can now perform a Q-twist hinged on the endpoints of α_2 and β_2 in $\sigma_2|_{H_2}$ and latched at vertices c_2^a and c_2^b. If this Q-Twist can be extended to all of G in σ_2, then we obtain an embedding σ_3 and then go to σ_1 as in Case 1. If not, then $\mathcal{A}_2 \neq \emptyset$. Let $H_3 = H_2 \cup (\bigcup \mathcal{A}_2)$, α_3 extends α_2 to the extreme attachments of $\mathcal{A}_2$ on $\gamma_{2n,1} \cup \gamma_{1,2}$, and β_3 extends β_2 similarly. Any H-bridge exterior to C_H in σ_2 with attachments producing an H-path that would cross some H-path of $\bigcup(\mathcal{B} \cup \mathcal{A}_1 \cup \mathcal{A}_2)$ if it were drawn exterior to C_H must be a reembedded bridge. Let $\mathcal{A}_3$ be the collection of such H-bridges. If $\mathcal{A}_3 = \emptyset$, we finish by extending to all of G a Q-Twist on $\sigma_2|_{H_3}$ hinged on the endpoints of α_3 and β_3 and latched at c_3^a and c_3^b and then refer to Case 1. If $\mathcal{A}_3 \neq \emptyset$, then we iterate this process again. Of course, this process must end as G is finite.

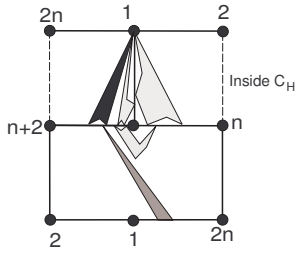

Figure 15.
An illustration of the iterative process: the light grey bridges are $\mathcal{B}$, the dark grey bridge is $\mathcal{A}_1$, and the black bridge is $\mathcal{A}_2$.

Case 3 Suppose $\sigma_1|_H = \sigma_2|_H = \nu_1$. Consider the faces of H as labeled in Figure 16.

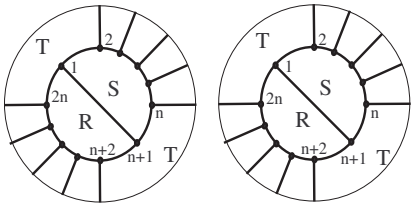

Figure 16.
Embeddings of H in Case 3

The only types of reembeddable bridges are those with all attachments on $\gamma_{1,2} \cup \gamma_{n,n+1}$ or all attachments on $\gamma_{2n,1} \cup \gamma_{n+1,n+2}$. Let $\mathcal{S}$ and $\mathcal{R}$, respectfully, be the collections of such bridges that are actually reembedded. If there is some reembedded bridge $B \in \mathcal{R} \cup \mathcal{S}$ which contains an H-path with both endpoints off of $\{v_2, v_n, v_{n+2}, v_{2n}\}$, then we may use this path to rechoose H so that we revert back to Case 2. Thus the reembedded bridges of $\mathcal{R} \cup \mathcal{S}$ form one or two fans (fans are described in Case 1) with apices in $\{v_2, v_n, v_{n+2}, v_{2n}\}$. So now all of the reembedding of G is happening within a 2-region Möbius strip with regions $\mathsf{R} \cup \mathsf{S}$ and T as in Case 1.2.3 with all reembedded bridges forming fans with apices in $\{v_2, v_n, v_{n+2}, v_{2n}\}$.

††When $\mathcal{S}$ is a set of sets, we use $\bigcup S$ to denote the union of the sets in $\mathcal{S}$.

The only difference between our current situation and Case 1.2.3 is that $\gamma_{1,n+1}$ cuts one region of the strip and that there may be fixed H-bridges attached to $\gamma_{1,n+1}$. However, $\gamma_{1,n+1}$ and any of these fixed bridges cannot interfere with the reembedding of the fans as described in Case 1.2.3. Thus we may take σ_1 to σ_2 as in Case 1.2.3.

Case 4 Suppose $\sigma_1|_H = \nu_1$ and $\sigma_2|_H = \nu_2$ (see Figure 17).

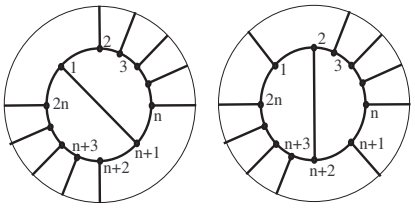

Figure 17.

Partition the reembedded (not just reembedable) bridges into two sets $\mathcal{B}_{in}$ and $\mathcal{B}_{out}$ for those that are interior and exterior, respectively, to C_H in σ_1. Note that any H-bridge with an attachment on the interior of $\gamma_{1,n+1}$ is in $\mathcal{B}_{in}$ and any H-bridge with an attachment in the interior of $\gamma_{2,n+2}$ is in $\mathcal{B}_{out}$. Suppose that B is an H-bridge with an attachment in the interior of $\gamma_{1,n+1}$. Then all of the other attachments of B are on exactly one of $\gamma_{1,2n}$, $\gamma_{1,2} \cup \gamma_{2,3}$, $\gamma_{n,n+1}$, $\gamma_{n+1,n+2} \cup \gamma_{n+2,n+3}$. Let $B_{1,2n}$, $B_{1,2,3}$, $B_{1,n}$, $B_{1,n+2,n+3}$, respectively, be the collections of these bridges with attachments on $\gamma_{1,n+1}$. Similarly bridges with attachments in the interior of $\gamma_{2,n+2}$ partition into the following four classes: $B_{2,1,2n}$, $B_{2,3}$, $B_{2,n+1,n}$, $B_{2,n+3}$.

Let B'_1 be the collection H-bridges with all attachments on $\gamma_{2n,1} \cup \gamma_{1,2}$. Let B'_{n+1} be the collection of H-bridges with all attachments $\gamma_{n,n+1} \cup \gamma_{n+1,n+2}$. Note $B'_1 \cup B'_{n+1} \subseteq \mathcal{B}_{out}$. Similarly, we define B'_2 and B'_{n+2}, where $B'_2 \cup B'_{n+2} \subseteq \mathcal{B}_{in}$.

Let $\mathcal{B}_1 = B_{1,2n} \cup B_{1,2,3} \cup B_{1,n} \cup B_{1,n+2,n+3} \cup B'_1 \cup B'_{n+1} \cup \gamma_{1,n+1}$ and $\mathcal{B}_2 = B_{2,1,2n} \cup B_{2,3} \cup B_{2,n+1,n} \cup B_{2,n+3} \cup B'_2 \cup B'_{n+2} \cup \gamma_{2,n+2}$. Now $\mathcal{B}_1 \cup \mathcal{B}_2 \subseteq \mathcal{B}_{in} \cup \mathcal{B}_{out}$ with equality being possible. Let $\mathcal{F}_{out} = \mathcal{B}_{out} \setminus (\mathcal{B}_1 \cup \mathcal{B}_2)$ and $\mathcal{F}_{in} = \mathcal{B}_{in} \setminus (\mathcal{B}_1 \cup \mathcal{B}_2)$. Without loss of generality, consider some $D \in \mathcal{F}_{in}$. The bridge D cannot have attachments on the interior of either $\gamma_{1,n+1}$ or $\gamma_{2,n+2}$; furthermore, D must have attachments on both $\alpha = \gamma_{2n,1} \cup \gamma_{1,2} \cup \gamma_{2,3}$ and $\beta = \gamma_{n,n+1} \cup \gamma_{n+1,n+2} \cup \gamma_{n+2,n+3}$ and these must be all of the attachments of D. Note now that either the only attachment of D on α is v_1 or the only attachment of D on β is v_{n+1} (assume the former) because otherwise D would cross $\gamma_{1,n+1}$ in σ_2. So now all such bridges in $\mathcal{F}_{in}$ have v_1 as their sole attachment on α, otherwise they would cross D in either σ_1 or σ_2 (depending on which side of the chord $\gamma_{1,n+1}$ they are on). Similarly, all bridges in $\mathcal{F}_{out}$ must have either v_2 as their sole attachment on α or v_{n+2} as their sole attachment on β.

Let α_1 be the subpath of α between the extreme endpoints of $\mathcal{B}_1$. Let β_1 be the subpath of β between the extreme endpoints of $\mathcal{B}_1$. Let $H_1 = H \cup (\bigcup \mathcal{B}_1)$. Any H-bridge exterior to C_H in σ_1 with attachments producing an H-path that would cross some H-path of $\mathcal{B}_1$ if it were drawn exterior to C_H must be a reembedded bridge. Let $\mathcal{A}_1$ be the collection of such H-bridges. We can now perform a Q-twist hinged on the endpoints of α_1 and β_1 in $\sigma_1|_{H_1}$ and latched at some vertex $c_1 \in \gamma_{1,n+1}$. If this Q-Twist can be extended to all of G in σ_1, then we obtain an embedding σ_3 for which $\sigma_3|_H = \nu_0$ and $\sigma_2|_H = \nu_2$ and then we can go from σ_3 to σ_2 by a sequence of Q-Twists as in Case 2. If we cannot perform this Q-Twist on all of G in σ_1, then $\mathcal{A}_1 \neq \emptyset$. In Figure 18, we have examples of where $\mathcal{B}_2 \cap \mathcal{A}_1 \neq \emptyset$ (the left configuration) and where $\mathcal{B}_2 \cap \mathcal{A}_1 = \emptyset$ (the right two configurations). Let $\widehat{\mathcal{A}}_1 = \mathcal{A}_1 \cup \mathcal{B}_2$ when $\mathcal{B}_2 \cap \mathcal{A}_1 \neq \emptyset$ and let $\widehat{\mathcal{A}}_1 = \mathcal{A}_1$ when $\mathcal{B}_2 \cap \mathcal{A}_1 = \emptyset$.

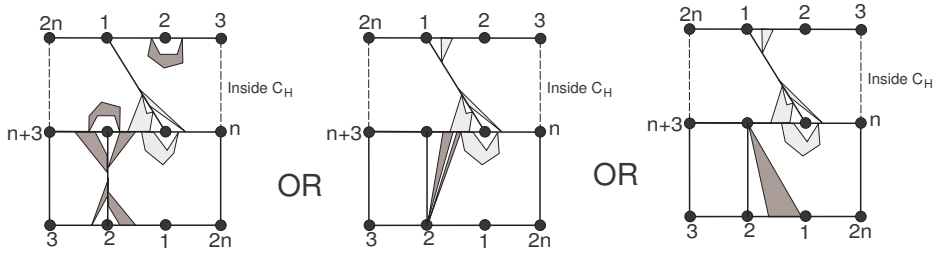

Figure 18.

Let $H_2 = H_1 \cup \left(\bigcup \widehat{\mathcal{A}}_1\right)$ and α_2 and β_2 extend α_1 and β_1 to the extreme attachments of $\widehat{\mathcal{A}}_1$ on α and β. Any H-bridge interior to C_H in σ_1 with attachments producing an H-path that would cross some H-path of $\bigcup(\mathcal{B}_1 \cup \widehat{\mathcal{A}}_1)$ if it were drawn interior to C_H must be a reembedded bridge. Let $\mathcal{A}_2$ be the collection of such bridges. In Figure 19, the black bridges in the first two configurations form $\mathcal{A}_2$ and in the third configuration we must have that $\mathcal{A}_2 = \emptyset$.

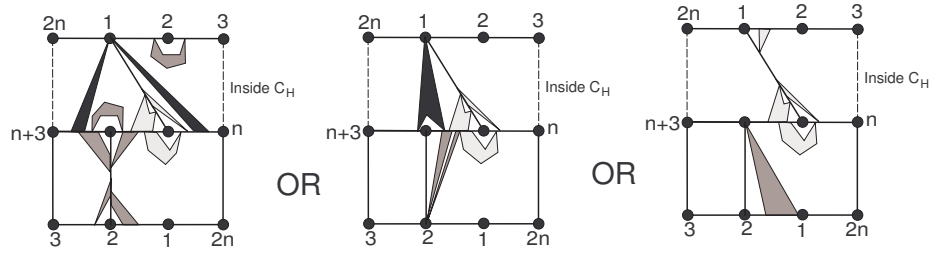

Figure 19.

We can now perform a Q-twist hinged on the endpoints of α_2 and β_2 in $\sigma_1|_{H_2}$ and latched at one or two vertices c_2^a and c_2^b. If this Q-Twist can be extended to all of G in σ_1, then we obtain an embedding σ_3 for which $\sigma_3|_H = \nu_0$ or ν_2 (depending on whether or not $\mathcal{B}_2$ is contained in $\widehat{\mathcal{A}}_1$ or not) and $\sigma_2|_H = \nu_2$ and then we can go from σ_3 to σ_2 by a sequence of Q-Twists as in Case 2 or Case 3. If we cannot perform this Q-Twist on all of G in σ_1, then $\mathcal{A}_2 \neq \emptyset$. If so, then let $H_3 = H_2 \cup (\bigcup \mathcal{A}_2)$ and α_3 and β_3 extend α_2 and β_2 to the extreme attachments of $\mathcal{A}_2$ on α and β. Any H-bridge exterior to C_H in σ_1 with attachments producing an H-path that would cross some H-path of $\bigcup(\mathcal{B}_1 \cup \widehat{\mathcal{A}}_1 \cup \mathcal{A}_2)$ if it were drawn exterior to C_H must be a reembedded bridge. Let $\mathcal{A}_3$ be the collection of such H-bridges. (In Figure 19, the first configuration must have $\mathcal{A}_3 = \emptyset$ but the second configuration may have $\mathcal{A}_3$ nonempty.) If $\mathcal{A}_3 = \emptyset$, we finish by extending to all of G a Q-Twist on $\sigma_2|_{H_3}$ hinged on the endpoints of α_3 and β_3 and latched at c_3^a and c_3^b and then refer to either Case 2 or Case 3. If $\mathcal{A}_3 \neq \emptyset$, then we define $\widehat{\mathcal{A}}_3$ similarly to $\widehat{\mathcal{A}}_1$ and iterate this process again. This process must end as G is finite.

Case 5: Suppose $\sigma_1|_H = \nu_1$ and $\sigma_2|_H = \nu_j$ for $3 \leq j \leq n-1$. See Figure 20. In Case 5.1 say that $n \geq 5$ and in Case 5.2 say that $n = 4$.

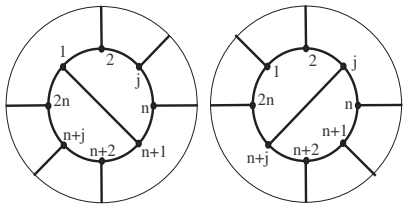

Figure 20.
Embeddings of H in Case 5

Case 5.1 Since $n \geq 5$, there are only two types of reembeddable bridges. Following similar notation as we did in Case 4, the first type of reembeddable bridges partition into the following 12 sets: $B_{1,2}$, $B_{1,2n}$, B'_1 and $B_{n+1,n}$, $B_{n+1,n+2}$, B'_{n+1} and $B_{j,j-1}$, $B_{j,j+1}$, B'_j, and $B_{n+j,n+j-1}$, $B_{n+j,n+j+1}$, B'_{n+j}. Say that

bridges in the first six sets *go along* with $\gamma_{1,n+1}$ and bridges from the second six sets go along with $\gamma_{j,n+j}$. The second type of reembeddable bridges partition into fans with apices from $\{v_1, v_2, v_n, v_{n+1}, v_{n+2}, v_{2n}\}$ or $\{v_{j-1}, v_j, v_{j+1}, v_{n+j-1}, v_{n+j}, v_{n+j+1}\}$. Say that bridges in fans with apex from the first set go along with $\gamma_{1,n+1}$ and bridges in fans with apex from the second set go along with $\gamma_{j,n+j}$.

So now in σ_1 all reembeddable bridges going along with $\gamma_{j,n+j}$ must be exterior to C_H except those in $B'_j \cup B'_{n+j}$ which are must be interior to C_H. Similarly, in σ_2 all reembeddable bridges going along with $\gamma_{1,n+1}$ must be exterior to C_H except those in $B'_1 \cup B'_{n+1}$ which must be interior to C_H. Therefore there is an embedding σ_3 of G with all bridges going along with $\gamma_{j,n+j}$ and all bridges going along with $\gamma_{1,n+1}$ exterior to C_H except the bridges in $B'_1 \cup B'_{n+1} \cup B'_j \cup B'_{n+j}$ which are all interior to C_H. Note that $\sigma_3|_H = \nu_0$ and so we go from σ_1 to σ_3 by a sequence of Q-Twists as in Case 2 and we go from σ_3 to σ_2 by a sequence of Q-Twists as in Case 2.

Case 5.2 Here $n = 4$ and so $\sigma_1|_H = \nu_0$ and and $\sigma_2|_H = \nu_3$. See Figure 21 for a different rendering of these embeddings. Recall that C_H is the octagon on $v_1v_2v_3v_4v_5v_6v_7v_8$ which is on the lower right in these figures.

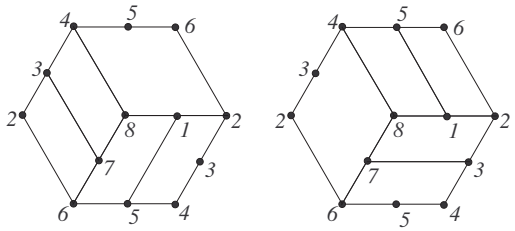

Figure 21.

In this case, a fixed H-bridge along with the fixed subgraph $\overline{H}$ need not actually be fixed pointwise in σ_1 and σ_2. This is because there may be H-bridges with all their attachments on $\gamma_{2,6} \cup \gamma_{4,8}$. So we do not use the terms fixed and reembedded in this case. We now partition the types of H-bridges that can exist in both embeddings of H into four different classes. First, a *singular bridge* is a single v_2v_4-, v_4v_6-, v_6v_8-, or v_2v_8-edge. For each of these singular bridges we say it has *corner vertex* v_3, v_5, v_7, or v_1, respectively. Second, a *corner bridge* has all attachments on two adjacent branches of H and is not a singular bridge. The branch vertex incident to both branches of a corner bridge is called the *corner vertex* of the bridge. Third, an *antipodal bridge* is a bridge that has all attachments on C_H that is not a corner bridge or a singular bridge. From Figure 21 we see that any antipodal bridge has all of its attachments on some $\gamma_{a,1+a} \cup \gamma_{4+a,5+a}$. Note that, by the maximality of V_8 among all V_{2n}-subdivisions in G, such a bridge cannot have attachments in the interiors of both $\gamma_{a,1+a}$ and $\gamma_{4+a,5+a}$ and that an antipodal bridge is exterior to C_H in both embeddings. Fourth, a *Petersen bridge* is not a corner bridge or singular bridge and either has an attachment in the interior of one of $\gamma_{2,6}$ and $\gamma_{4,8}$ or has all of its attachments on at least three vertices from $\{v_2, v_4, v_6, v_8\}$. Note that a Petersen bridge is always exterior to C_H in both embeddings with all attachments on $\gamma_{2,6} \cup \gamma_{4,8}$. Further note that it is impossible to have both an antipodal bridge and a Petersen bridge, as both are exterior to C_H in both embeddings.

We split the remainder of this case into five subcases. In Case 5.2.1 we say that there is a Petersen bridge with attachments in the interiors of both $\gamma_{2,6}$ and $\gamma_{4,8}$. If there is no Petersen bridge having attachments in the interiors of both $\gamma_{2,6}$ and $\gamma_{4,8}$, then without loss of generality we can say that in Case 5.2.2 that there is a Petersen bridge with attachments v_4, v_8, and v_9 where v_9 is an interior vertex of $\gamma_{2,6}$, in Case 5.2.3 that there is a Petersen bridge attached at v_8 and v_9 where v_9 is an interior vertex of $\gamma_{2,6}$, in Case 5.2.4 that there is a Petersen bridge having three or four attachments all of which are from $\{v_2, v_4, v_6, v_8\}$, and in Case 5.2.5 that there is no Petersen bridge. In Cases 5.2.1–5.2.4 let B denote the Petersen bridge identified.

Case 5.2.1 There is an H-path in B whose union with H forms a subdivision of the Petersen graph, call this subdivision P. Rechoose P so that it has no local bridges and the same branch vertices. There

are two distinct labeled embeddings of P in the projective plane (a fact one can check or see [18]) and we claim that $\sigma_1|_P \neq \sigma_2|_P$. If we assume that $\sigma_1|_P = \sigma_2|_P$, then since any embedding of P has representativity 3, any P-bridge belongs to a unique face of P and so by 3-connectivity the embedding of a P-bridge in its face is unique up to isotopy and so $\sigma_1 = \sigma_2$, a contradiction.

Now, one can check that any P-bridge in G must have all of its attachments on two adjacent branches of P in order to belong to a face of both embeddings of P. Again we now have a unique corner vertex of P for any P-bridge. One can also check that for any uv-branch of P, that the corner bridges for u and the corner bridges for v do not overlap along the uv-branch or else they will cross in either σ_1 or σ_2. Thus we can go from σ_1 to σ_2 by a P-Twist or a degenerate P-Twist.

Case 5.2.2 Here $H \cup B$ again contains a Petersen graph subdivision and we finish as in Case 5.2.1.

Case 5.2.3 Here $H \cup B$ contains a subdivision of the 1-edge contraction of the Petersen graph, call it P', where $\sigma_1|_{P'}$ and $\sigma_2|_{P'}$ are as shown in Figure 22. Note that any P'-bridge is either an H-bridge or has attachments on the interior of the v_8v_9-branch of P'. Let $\mathcal{H}$ and $\mathcal{P}'$ be the collections of these two types of P'-bridges. The v_8v_9-branch may now be rechosen as in [9, 6.2.1] so that there are no local P'-bridges on the v_8v_9-branch and so since H has no local bridges, neither does P'.

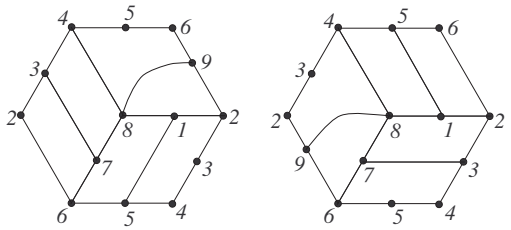

Figure 22.

Recall that there can be no antipodal bridges in $\mathcal{H}$ and so any bridge in $\mathcal{H}$ is either a corner bridge or a singular bridge. Furthermore any corner bridge at v_8 must have all of its attachments on $\gamma_{1,8} \cup \gamma_{7,8}$. Any bridge in $\mathcal{P}'$ is either a corner bridge with corner vertex v_9 or has all attachments on $\gamma_{4,8} \cup \gamma_{8,9}$. Thus there is a 1-edge decontraction G' of G at v_8 which extends the embeddings σ_1 and σ_2 to σ_1' and σ_2' analogous to what is shown in Figure 23. Note that the figure depicts only corner bridges at v_8 and not singular bridges. However, any singular bridge that may exist can be assigned to either v_8 or v_8' as needed. So now G' contains a subdivision of the Petersen graph and is 3-connected and so σ_1' and σ_2' are related by a single P-Twist as in Case 5.2.1. Thus σ_1 and σ_2 are related by this same P-Twist or a P-Twist obtained by a contraction of it.

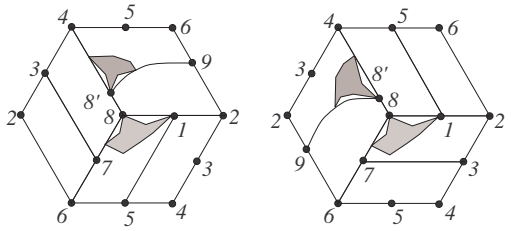

Figure 23.

Case 5.2.4 Here $H \cup B$ contains a subdivision of the 1-edge contraction of the Petersen graph and so we finish as in Case 5.2.3.

Case 5.2.5 If there are no singular H-bridges, then since there are no Petersen bridges, then any H-bridge that is interior to C_H in both σ_1 to σ_2 or exterior to C_H in both σ_1 to σ_2 is fixed pointwise (up to isotopy) with respect to $\overline{H}$ and so we finish as in Case 5.1. So assume there are singular bridges. Either there is a singular bridge that is exterior to C_H in both embeddings or not. If not, then, similarly, any H-bridge that is interior to C_H in both σ_1 to σ_2 or exterior to C_H in both σ_1 to σ_2 is fixed pointwise (up to isotopy) with respect to $\overline{H}$ and so we finish as in Case 5.1. If so, then assume, without loss of

generality, that the singular bridge is a v_6v_8-edge. Let H' be the union of H and the v_6v_8-edge. So $\sigma_1|_{H'}$ and $\sigma_2|_{H'}$ are as shown in Figure 24.

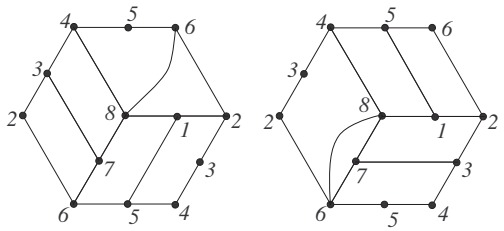

Figure 24.

Now in this case, we can perform a 1-edge decontraction of G at v_8 similar to Case 5.2.3 that extends the embeddings. Again we get that σ_1 and σ_2 are related by a single P-Twist.

5 Proof of Lemma 1.2 for V_8-free graphs

In this section, we will prove Lemma 1.2 in the case where G is V_8-free. Formally, we assume that G is 3-connected and V_8-free and has two embeddings σ_1 and σ_2 in the projective plane. We will show that these two embeddings are related by Q-Twists and P-Twists. We use Theorem 1.3 which characterizes internally 4-connected graphs with no V_8-minor. Hence we need to analyze the 3-separations of G to reduce to an internally 4-connected sub-structure in G. Two degenerate cases are where G is a 3-sum of two planar graphs (Section 5.1) and G is a 3-sum of two non-planar graphs (Section 5.2). The main analysis comes in Section 5.3.

5.1 A 3-sum of two planar graphs

Let G be a 3-connected, non-planar graph that is embedded in the projective plane and G not internally 4-connected. Then there is a 3-sum $G = G_1 \oplus_3 G_2$. In this section we will prove Lemma 1.2 for the case for which G_1 and G_2 are both planar. The proof follows from Propositions 5.1 and 5.2. (We actually do not use the assumption that G is V_8-free in this section.)

Recall that a cycle in a graph is *peripheral* if it is chordless and non-separating. Also recall that in a 3-connected planar graph the peripheral cycles are exactly the facial cycles.

Proposition 5.1. *Suppose G is 3-connected, projective planar, nonplanar, and $G = G_1 \oplus_3 G_2$ where both G_1 and G_2 are planar. Then the triangle of summation is non-peripheral in at least one of G_1 and G_2. Furthermore, $G = K_3 \oplus_3 H_1 \oplus_3 H_2 \oplus_3 \cdots \oplus_3 H_k$ where $3 \leq k \leq 4$, each H_i is planar and summed into K_3, and the triangle of summation is peripheral in H_i.*

Proof. If the triangle of summation in $G_1 \oplus_3 G_2$ is peripheral in both, then $G = G_1 \oplus_3 G_2$ is planar, a contradiction. Supposing the triangle is not peripheral in G_1, we get that $G = K_3 \oplus_3 G_{1,1} \oplus_3 G_{1,2} \oplus_3 G_2$ where the sums are all at K_3. Repeating this process we get that $G = K_3 \oplus_3 H_1 \oplus_3 H_2 \oplus_3 \cdots \oplus_3 H_k$ in which each H_i is planar with its triangle of summation being peripheral and $k \geq 3$. We cannot have that $k \geq 5$ because then G will contain a $K_{3,5}$-minor, which is not projective planar, a contradiction. □

Consider the six embeddings shown on the left in Figure 25. Ignoring the shaded triangles, one can check that these six embeddings are all of the embeddings of $K_{3,3}$ in the projective plane. Each arrow represents a Q-Twist between the two embeddings at its ends. For example, to change the embedding at the top of the figure to the adjacent one clockwise to it, use a Q-twist hinged at $1, 3, b, c$ and latched at a. Similarly on the right of Figure 25 we show all of the embeddings and Q-Twists between them for $K_{3,4}$.

Proposition 5.2. *If $G = K_3 \oplus_3 H_1 \oplus_3 H_2 \oplus_3 \cdots \oplus_3 H_k$ is as in Proposition 5.1 and σ_1 and σ_2 are two embeddings of G in the projective plane, then we can go from σ_1 to σ_2 by a sequence of Q-Twists.*

Proof. Given $G = K_3 \oplus_3 H_1 \oplus_3 H_2 \oplus_3 \cdots \oplus_3 H_k$ as in Proposition 5.1. If $k = 3$, then G contains a subdivision H of $K_{3,3}$ with H-bridges as shown on the left in Figure 25 and so G has the six embeddings in the projective plane as shown. The arrows now represent Q-Twists that are modified from the ones for $K_{3,3}$. For example, to change the embedding at the top to the one the adjacent one clockwise to it, use a Q-twist hinged at b, c, and two cut-vertices on the $(a,1)$-path and $(a,3)$-path and latched at a. For $k = 4$, G contains a subdivision H of $K_{3,4}$ and we get the structure and embeddings of G as shown on the right of Figure 25. These are related by the same Q-twists as in the case where $k = 3$. □

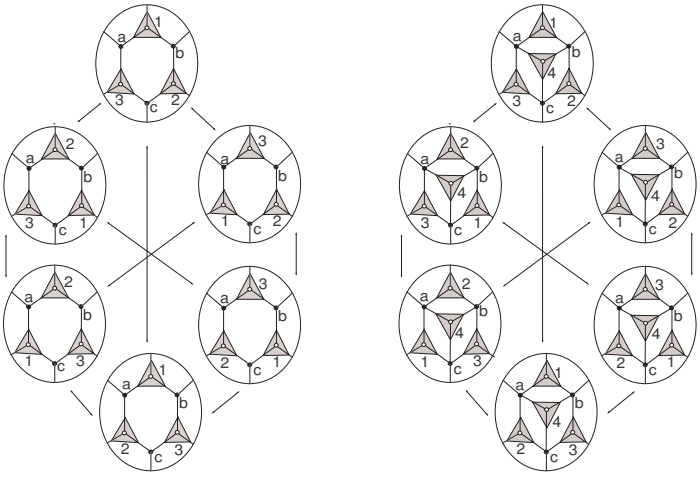

Figure 25.

5.2 A 3-sum of two non-planar graphs

In this section we prove Lemma 1.2 for the case that G is a 3-sum of two nonplanar graphs. The proof follows from Proposition 5.3. (We actually do not use the assumption that G is V_8-free in this section.)

Proposition 5.3. *If G is 3-connected and $G = G_1 \oplus_3 G_2$ where each G_i is nonplanar, then we can go from any one embedding of G in the projective plane to any other embedding by a sequence of Q-Twists.*

Proof. Since each G_i is nonplanar and 3-connected, either $G_i \cong K_5$ or G_i contains a $K_{3,3}$-subdivision. From [17, 10.3.9], if G_i contains a $K_{3,3}$-subdivision, then G_i contains a minor from Figure 26 where the triangle of summation of G_i is shown in bold. Call the left-hand graph T_1 and the right-hand graph T_2.

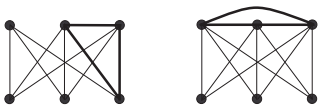

Figure 26.

Neither G_1 nor G_2 can contain a T_2-minor because then if the other term is isomorphic to K_5 or contains either a T_1- or T_2-minor it will imply that $G = G_1 \oplus_3 G_2$ contains a $K_{3,5}$-minor. This makes G not projective planar, a contradiction. Thus for each i, $G_i \cong K_5$ or G_i contains a T_1-minor.

If $G_1 \cong G_2 \cong K_5$, then $G = G_1 \oplus_3 G_2$ consists of $K_{3,4}$ along with two additional edges that connect pairs of 3-valent vertices, and possibly some edges of a triangle on the 4-valent vertices. Let $\widehat{K}_{3,4}$ be the graph obtained from $K_{3,4}$ by adding $(1,2)$- and $(2,4)$-edges. Since $K_{3,4}$ has the six embeddings as described before, the embeddings of $\widehat{K}_{3,4}$ are obtained from these six embeddings. On the left of Figure 27, we show these six embeddings of $\widehat{K}_{3,4}$. The arrows between the embeddings correspond to Q-Twists similar to those in Proposition 5.2. In the middle of Figure 27, we show the four embeddings of $\widehat{K}_{3,4}$

that allow the (a,b)-edge. This (a,b)-edge has two possible placements shown by dashed lines in the figure. Again, the flexibilities are obtained by similar Q-Twists and flipping of the (a,b)-edge. Finally, on the right of Figure 27, we show the two embeddings of $\widehat{K}_{3,4}$ that allow the (a,b)-edge and (b,c)-edge. These two edges each have two possible placements shown by dashed lines in the figure. Again, these are related by Q-Twists and flipping of the (a,b)- and (b,c)-edges. It is not possible to embed all three edges of the triangle $\{a,b,c\}$.

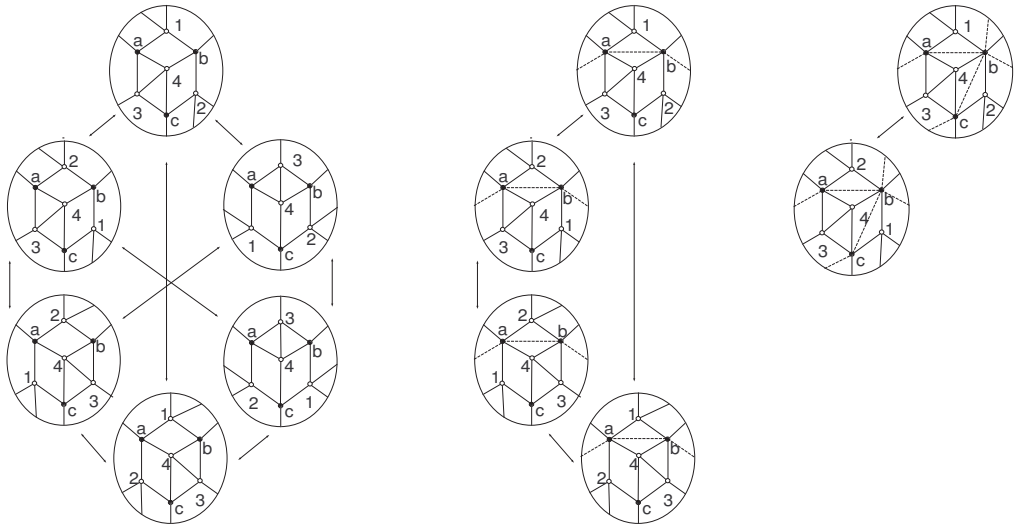

Figure 27.

So now we may assume without loss of generality that G_1 contains a T_1-minor. Label the vertices of $K_{3,4}$ as $v_a, v_b, v_c, v_1, v_2, v_3, v_4$ as in Figure 25. Now if $G_2 \cong K_5$, then G contains a minor isomorphic to the graph obtained from $K_{3,4}$ by a single split at vertex v_a leaving a 3-separation with v_1 and v_2 on one side and v_3 and v_4 on the other side. Call this graph S_1. We get the similar result when G_2 has a T_1-minor and the two minors in G_1 and G_2 are summed with the 3-valent vertices on the triangle of summation identified. If G_1 and G_2 both have T_1-minors and the sum does not have the 3-valent vertices coinciding, then G contains a minor isomorphic to the graph obtained from $K_{3,4}$ by splits at v_a and at v_b that leave a 3-separation with v_1 and v_2 on one side and v_3 and v_4 on the other side. Call this graph S_2. Note that if we split the third 4-valent vertex of $K_{3,4}$ in a way that preserves the separation of v_1, v_2 from v_3, v_4, then we obtain a graph that is an excluded minor for projective planarity. So we split the remainder of the proof into two cases: in Case 1, G contains an S_1-subdivision as described and in Case 2, G contains an S_2-subdivision as described. In each case we assume that $v_1, v_2 \in G_1$ and $v_3, v_4 \in G_2$.
Case 1 Of the six embeddings of $K_{3,4}$ (see Figure 25) there are four that extend to embeddings of S_1. The bottom and lower left embeddings in Figure 25 do not extend. By symmetry we need only show how to go from the embedding of G with the embedding of S_1 corresponding to the top embedding in Figure 25 to an embedding of G with the embedding of S_1 given by one of the other three.

For each of the three cases, Figure 28 shows all of the possible S_1-bridges that can occur in both embeddings of S_1 with 3-separation of G at $v_{a''}, v_b, v_c$. Bridges around the split vertex v_a are shown in lighter colors. The reader can check that no other S_1-bridges are possible. In the first case, we go from the first embedding to the second by a degenerate Q-Twist hinged at $v_{a''}, v_c$ and latched at v_b. In the second case, we go from the first to the second embedding by a Q-twist hinged at $v_{1'}, v_b, v_{3'}, v_c$ and latched at $v_{2'}, v_{4'}$. In the third case, we go from the first embedding to the second embedding by a degenerate P-Twist obtained from the central view of the P-Twist (see Figure 3) with v_4 in the center patch 7, the patches 0 and 9 contracted to make v_b, and patches 3 and 4 contracted to make v_c.

Figure 28.

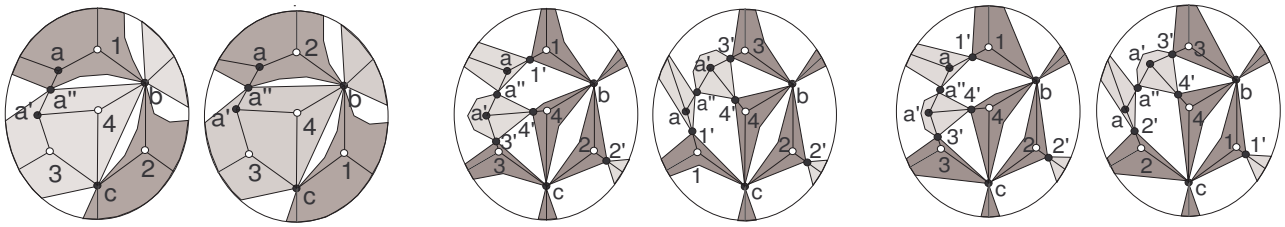

Case 2 Of the six embeddings of $K_{3,4}$ (see Figure 25) there are two that extend to embeddings of S_2. They are the two embeddings on the right in Figure 25. The possible S_2-bridges that can occur in both embeddings of S_2 all fall into the shaded regions of Figure 29. (Recall that edge from the split at vertex v_a and the edge from the split at vertex v_b are on separate sides of the 3-separation.)

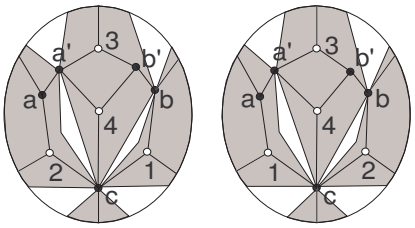

Figure 29.

So now we can go from the first embedding to the second by a degenerate Q-Twist hinged at $v_{a'}$ and b and latched at v_c. □

5.3 Reduction to an internally 4-connected frame

In this section we prove Lemma 1.2 for the case that G is V_8-free and cannot be written as a 3-sum of two planar or two nonplanar terms. A 3-connected nonplanar graph G admits a *patch decomposition* with an internally 4-connected *frame* F_G and *patches* P_i when either G is internally 4-connected (and is its own frame with no patches) or $G = F_G \oplus_3 P_1 \oplus_3 P_2 \oplus_3 \cdots \oplus_3 P_k$ where

- F_G is an internally 4-connected non-planar graph,
- each P_i is planar and summed into a triangle of F_G,
- the triangle of summation is peripheral in P_i,
- no three P_i are summed into the same triangle of F_G.

.

Proposition 5.4. *If G is 3-connected, nonplanar, and G cannot be written as a 3-sum of two planar or two nonplanar terms, then G admits a patch decomposition or any two embeddings of G are related by a sequence of Q-Twists.*

Proof. We proceed by induction on $|V(G)|+|E(G)|$. In the base case $|V(G)|+|E(G)| = 15$ and $G = K_5$ or $K_{3,3}$ and our result is immediate. So now say that $|V(G)|+|E(G)| > 15$. If G is internally 4-connected, then we have our result. If not, then write $G = G' \oplus_3 P$ where the summation is along triangle T and $|E(P)| \geq 4$. By assumption G' is nonplanar and P is planar. Rechoose G' and P so that the number of vertices in P is maximal. If T is not peripheral in P, then because P is planar we get that $P = P_1 \oplus_3 P_2$ where the 3-sum is on T and T is peripheral in each P_i.

Either G' cannot be written as a 3-sum of two planar or two nonplanar terms or it can. Let these be Case 1 and Case 2.

Case 1 By the inductive hypothesis, we then get that $G' = F_{G'} \oplus_3 Q_1 \oplus_3 Q_2 \oplus_3 \cdots \oplus_3 Q_m$ as stated in our desired result. Let T_i be the triangle in $F_{G'}$ along which the summation with Q_i is taken. By the maximality of P and the fact that G is not a 3-sum of two nonplanar graphs, it must be that T is a triangle of $F_{G'}$ and is not on the same vertices of any T_i. Thus either $G = F_{G'} \oplus_3 Q_1 \oplus_3 Q_2 \oplus_3 \cdots \oplus_3 Q_m \oplus P$ or $G = F_{G'} \oplus_3 Q_1 \oplus_3 Q_2 \oplus_3 \cdots \oplus_3 Q_m \oplus P_1 \oplus_3 P_2$ satisfies our desired conclusion.

Case 2 We assume that $G' = G_1 \oplus_3 G_2$ where G_1 and G_2 are both planar or both nonplanar. (Assume that $T \subset G_2$.) It cannot be the latter case because then $G = G_1 \oplus_3 (G_2 \oplus_3 P)$ where G_1 and $G_2 \oplus_3 P$ are both nonplanar, a contradiction. If both G_1 and G_2 are planar, then rechoose G_1 and G_2 so that there is a maximum number of vertices in G_1 and $T \subset G_2$. Let T' be the triangle of summation for $G_1 \oplus_3 G_2$. Note that since G is not a 3-sum of two planar terms, it must be that $G_2 \oplus_3 P$ is nonplanar. Hence T is nonperipheral in either G_2 or P. If T is nonperipheral in G_2 and peripheral in P, then $G_2 = G_2' \oplus_3 G_2''$ summed along T and where T' is in G_2'. Thus $G = (G_1 \oplus_3 G_2') \oplus_3 (G_2'' \oplus_3 P)$ where $(G_2'' \oplus_3 P)$ is planar. This contradicts the maximality of P. So it must be that T is not peripheral in P and $G = G_1 \oplus_3 G_2 \oplus_3 (P_1 \oplus_3 P_2)$ (see Figure 30). By a similar argument the maximality of G_1 implies that T' is nonperipheral in G_1 and hence $G_1 = H_1 \oplus_3 H_2$ along T' which makes $G = (H_1 \oplus_3 H_2) \oplus_3 G_2 \oplus_3 (P_1 \oplus_3 P_2)$. In Cases 2.1, 2.2, 2.3, and 2.4 say that $|V(T) \cap V(T')| = 0$, 1, 2, and 3, respectively. In all three cases, let $V(T) = \{a, b, c\}$ and $V(T') = \{a', b', c'\}$.

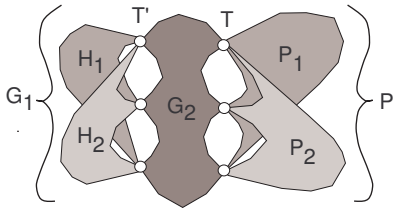

Figure 30.

Case 2.1 The graph M constructed by taking two vertex-disjoint copies of $K_{2,3}$ and connecting the 3-partite sets by three edges is one of the 35 excluded minors for projective-planar graphs. Since G_2 must be 3-connected, there are three vertex-disjoint paths linking $V(T)$ to $V(T')$. Thus G has an M-minor, a contradiction.

Case 2.2 Say that $V(T) \cap V(T') = \{c\}$. Since G_2 is 3-connected, there are disjoint paths in $G_2 \backslash c$ linking $\{a, b\}$ and $\{a', b'\}$ (assume without loss of generality that these two paths link a to a' and b to b') and so G contains as an S_2-subdivision, call it S. The two embeddings of S_2 are shown in Figure 29. So in this case, the S-bridges in G fall into the shaded regions shown in Figure 31 where the S-bridges in G_2 are shown in darker grey. Any S-bridge in $H_1 \cup H_2 \cup P_1 \cup P_2$ is fixed pointwise up to isotopy with respect to a fixed embedding of S_2; however, the bridges in G_2 each may have up to two possible placements in two of the dark shaded regions. Thus the configuration of the bridges in G_2 and their possible reembeddings are as described in Case 1.2.3.1 of Section 4 where the reembeddings are shown to be related to each other by sequences of Q-Twists. The two reembeddings of the S_2-subdivision are related to each other by a single Q-Twist hinged on a', b' and latched at c.

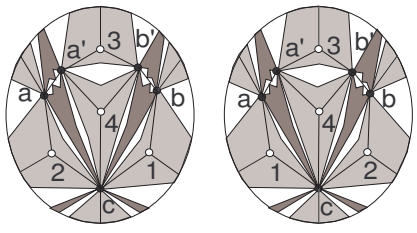

Figure 31.

Case 2.3 Say that $V(T) \cap V(T') = \{b, c\}$. In this case G contains an S_1-subdivision, call it S, rooted on $\{a, a', b, c\}$ and with 3-valent vertices $v_1 \in P_1$, $v_2 \in P_2$, $v_3 \in H_1$, $v_4 \in H_2$. Of the six embeddings of $K_{3,4}$ shown in Figure 25 with corresponding labels, only four allow the decontraction to S_1. The bottom and bottom left embeddings of $K_{3,4}$ do not extend to S_1.

Now if v is a vertex in $G_2 \setminus \{a, a', b, c\}$, then by 3-connectivity there are three internally-disjoint paths in G_2 connecting v to $\{a, a', b, c\}$. In the four possible embeddings of S_1, the only possibilities are that v is linked to $\{a, a', b\}$ or $\{a, a', c\}$. Furthermore, if v links to $\{a, a', c\}$, then no other vertex in $G_2 \setminus \{a, a', b, c\}$ links to $\{a, a', b\}$.

If there are vertices in $G_2 \setminus \{a, a', b, c\}$ and they all link to $\{a, a', b\}$, then there are two possible embeddings of S with all of the S-bridges falling into the shaded regions shown on the left of Figure 32. Similar to Case 2.2 above, the S-bridges in $H_1 \cup H_2 \cup P_1 \cup P_2$ are fixed with respect to a fixed embedding of S_1 but the bridges in G_2 each have up to two possible placements. So as in the previous case, any two embeddings of G are related by a sequence of Q-Twists.

If there are vertices in $G_2 \setminus \{a, a', b, c\}$ and they all link to $\{a, a', c\}$, then the embeddings of S are as shown on the right in Figure 32 with S-bridges in the shaded regions. Similar to what is explained in the previous paragraph, any two embeddings of G are related by a Q-Twist

Figure 32.

If there are no vertices in $G_2 \setminus \{a, a', b, c\}$, then the S-bridges of G are all corner bridges cornered at v_1, v_2, v_3, v_4 which are all fixed pointwise with respect to a given embedding of the S_1-subdivision save for single-edge bridges on $\{a, a', b, c\}$. So since there are four embeddings of S in the projective plane, all embeddings of G are shown in Figure 33 up to flexibility of single edges (which is accounted for by degenerate Q-Twists). The first embedding goes to the second by a Q-Twist hinged at a', c and latched at b. The first embedding goes to the third by a Q-Twist hinged at b, c and latched at a, a' (the bridges in the twisted patch is shown in darker grey). The third embedding goes to the fourth by a Q-Twist hinged at a', b and latched at c.

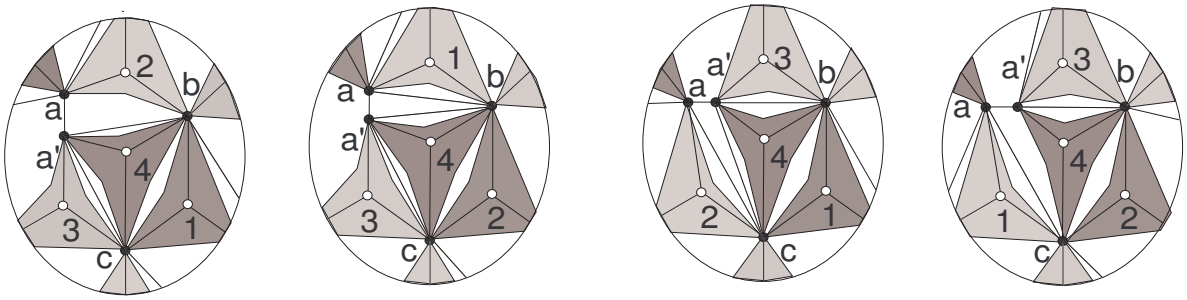

Figure 33.

Case 2.4 Here we must have that $|V(G_2)| = 3$ because otherwise G will contain a $K_{3,5}$-minor, a contradiction of projective planarity. However now if $|V(G_2)| = 3$, then $G = G_1 \oplus_3 P$ where both G_1 and P are planar, a contradiction. □

Now consider a 3-connected nonplanar graph G that has a patch decomposition $F_G \oplus_3 P_1 \oplus_3 P_2 \oplus_3 \cdots \oplus_3 P_k$. Note that F_G is a minor of G by 3-connectivity and the definition of 3-summing. (We do not consider a Y-Delta operation to be a 3-sum.) If G is embedded in the projective plane, then the patch decomposition naturally yields a unique embedding (up to flipping single edges in F_G that are not in G) of F_G with triangular shaded patches in the places of the P_i's. Similarly such a patch embedding of F_G corresponds to a unique embedding of G. So now let ψ_1 and ψ_2 be two embeddings of G and σ_1 and σ_2 associated patch embeddings with flexible single edges placed arbitrarily. Thus if we can explain how to go from σ_1 to σ_2 by Q-Twists and P-Twists, then we will have explained how to go from ψ_1 to ψ_2 by Q-Twists and P-Twists. Thus Theorem 5.5 suffices to complete the proof of Lemma 1.2 for the case where G is V_8-free.

Theorem 5.5. *If G is 3-connected, nonplanar, V_8-free, and has a patch decomposition, then we can go from σ_1 to σ_2 by a sequence of Q-Twists and P-Twists.*

The proof of Theorem 5.5 begins as follows. Since G does not contain a V_8-minor, neither does F_G (because F_G is a minor of G) and so Theorem 1.3 yields cases for the exact structure of F_G. In Section 5.3.1, we assume that F_G has five vertices; in Section 5.3.2, F_G is a double wheel; in Section 5.3.3, F_G has six vertices; in Section 5.3.4, F_G has seven vertices; in Section 5.3.8, F_G is 4-vertex coverable; and in Section 5.3.9, $F_G \cong L(K_{3,3})$.

5.3.1 Frames on five vertices

Given that F_G has five vertices and is nonplanar, we get that $F_G \cong K_5$. There are 27 distinct labeled embeddings of K_5 on the projective plane. Twelve of the 27 have a facial 5-cycle and the remaining 15 do not (see Figure 34).

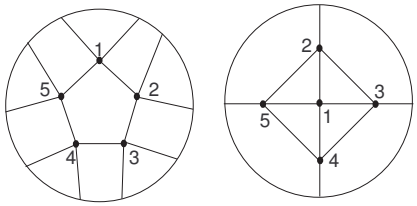

Figure 34.

Denote the embedding with facial 5-cycle a, b, c, d, e by $\sigma_{(abcde)}$. We need not consider the 15 embeddings without a facial 5-cycle by the following argument. If σ_1 is as in the right of Figure 34, then because edges $(2, 3)$ and $(4, 5)$ form the diagonals of quadrilateral face $(3, 5, 2, 4)$, at least one of $(2, 3)$ or $(4, 5)$ can be flipped across the boundary by a degenerate Q-Twist because there can be at most two triangular patches in the face $(3, 5, 2, 4)$. Thus we obtain a new patch embedding σ_1' with K_5 having a facial 5-cycle. So for the remainder of this section, we assume that both σ_1 and σ_2 are facial 5-cycle type embeddings.

Of the 12 embeddings of K_5 with a facial 5-cycle, the patches fall into two types: *outside patches* have their attachments on one of the 5 triangular faces of K_5 and *inside patches* that do not. Outside patches may be embedded in either the interior or exterior of the pentagon, while inside patches must be embedded in the interior. Therefore, if a double patch occurs, then they are outside patches. In Case 1 say there is a double patch and in Case 2 there is not. Note that there cannot be two sets of double patches.

Case 1 Assume the double patch is on the vertices $(1, 2, 3)$. These two triangular patches are embedded so that they meet at an edge and at the antipodal vertex from that edge on the 5-face. Moreover, either they meet in the same edge of triangle $(1, 2, 3)$ in both σ_1 and σ_2 or not. Without loss of generality in

Case 1.1, the two patches meet at the $(2,3)$-edge in both σ_1 and in σ_2 and in Case 1.2, the patches meet at $(2,3)$ in σ_1 and at $(1,3)$ in σ_2.

Case 1.1 Either the cyclic order along the 5-cycle is the same or the vertices 4 and 5 have been transposed. If they are the same, it is clear that the embeddings are identical. The pair of embeddings with 4 and 5 transposed are shown on the left in Figure 35 with all possible patches included. The Q-Twist latched at 1 and hinged at 2 and 3 takes one embedding to the other.

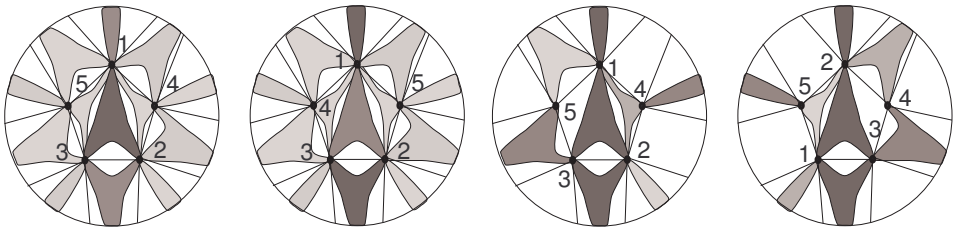

Figure 35.
K_5-Frames with a double patch - Case 1 is a Q-Twist while Case 2 is a P-Twist

Case 1.2 We can assume that the first embedding of the frame is $\sigma_{(14235)}$, while the second is either $\sigma_{(15243)}$ or $\sigma_{(14253)}$. The first possibility with all possible patches included is shown on the right of Figure 35. This pair of embeddings can be seen to be related by a degenerate P-Twist as follows: from the patch structure in Figure 3, contract patches 0 and 8 to form node 1, contract patches 2 and 7 to form node 2, contract patch 5 to form node 3, the intersection of patches 4 and 6 form node 4 and the intersection of patches 3 and 4 form node 5 (this actually describes the P-Twist that takes the second embedding to the first). If the second possibility occurs, then a Q-Twist on latched at 2 and hinged at 1 and 3 will take the embeddings to the first possibility.

Case 2 Now we assume that there are no double patches on the K_5-frame. It is possible that an outside patch may be embedded inside the pentagonal face. Since the patch is not doubled, however, it may be moved outside the pentagonal face by a degenerate Q-Twist. So we can assume that all outside patches are actually embedded outside the pentagonal face.

Without loss of generality we can assume that $\sigma_1 = \sigma_{(12345)}$. This is shown in the center of Figure 36. We can obtain the other 11 pentagonal embeddings of K_5 from $\sigma_{(12345)}$ by performing any permutation on 1,2,3,4,5 and then rotating so that vertex 1 is at the top and then possibly reflecting around a vertical axis through vertex 1. There are 10 2-cycle permutations in S_5 and these give rise to five distinct embeddings which are shown at a distance 1 from the center of Figure 34. There are 10 3-cycle permutations in S_5 and these give rise to another five distinct embeddings which are shown at a distance two from the center of Figure 34. The remaining two permutations in S_5 give the one remaining embedding, $\sigma_{(14253)}$. Since we have now accounted for all 12 pentagonal embeddings and have shown symmetry by 2-cycle and 3-cycle permutations, we can split the remainder of the proof in this section into four subcases: in Case 2.1, $\sigma_2 = \sigma_1$; in Case 2.2, the permutations of σ_1 and σ_2 differ by a 2-cycle permutation; in Case 2.3, the permutations of σ_1 and σ_2 differ by a 3-cycle permutation; and in Case 2.4, $\sigma_2 = \sigma_{(14253)}$.

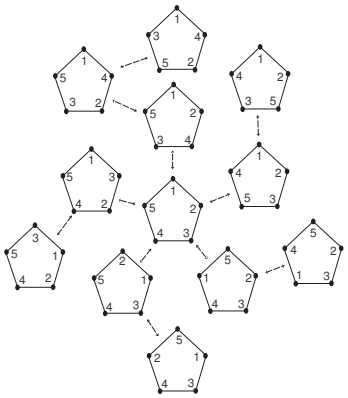

Figure 36.

In each case, we will find all of the maximal sets of patches that embed in both frame embeddings and then show how the two embeddings are related by a sequence of (degenerate) Q-Twists or P-Twists. Note that given two patches that could possibly embed in a given frame embedding, they can embed simultaneously unless they are both inside bridges and they share consecutive attachments along the 5-cycle.

Relative to the two frame embeddings, there are: *In-In patches* that are inside patches in both embeddings of K_5, *In-Out patches* that are inside patches in σ_1 and outside patches in σ_2, *Out-In Patches*, and *Out-Out Patches*.

Case 2.1 Once any patch in the interior of the 5-cycle that can be reembedded on the outside has been moved out by a degenerate Q-Twist, all the other patches must be fixed. Hence the embeddings are identical.

Case 2.2 By renumbering and reflecting around the vertical axis, we can assume that $\sigma_2 = \sigma_{(12354)}$. Since outside patches have been moved to the exterior to the pentagon, we can assume that all Out-Out patches (i.e. $(1,3,4), (1,3,5)$ and $(2,4,5)$) exist.

There are three possible In-In patches, $(1,2,3)$, $(3,4,5)$, and $(1,4,5)$. In Case 2.2.1, say that the $(1,2,3)$-patch exists and in Case 2.2.2 say that it does not.

Case 2.2.1 Neither of the In-Out patches $(2,3,4)$ nor $(1,4,5)$ can exist in both σ_1 and σ_2 as they are blocked by the $(1,2,3)$-patch. Similarly, the Out-In Patches $(2,3,5)$ and $(1,2,4)$ cannot exist. Finally either of the remaining In-In patches $(3,4,5)$ and $(1,4,5)$ can exist, but not both simultaneously. Hence there are only two maximal patch structures in this case (and they are symmetric). See Figure 37. Note that a Q-Twist hinged at $1,3,4,5$ and latched at 1 and 3 will take one embedding to the other.

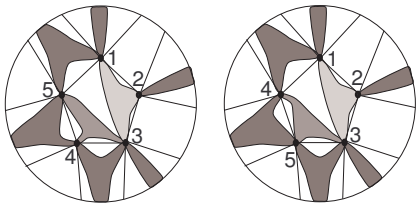

Figure 37.
$\sigma_{(12345)}$ and $\sigma_{(12354)}$ with In-In patches $(1,2,3)$ and $(3,4,5)$ - Related by a Q-Twist

Case 2.2.2 Here either the $(3,4,5)$-patch or $(1,4,5)$-patch may exist, but not both simultaneously. By symmetry we either have that the $(3,4,5)$-patch exists or there is no In-In patch.

In the first case, the only admissible patches are $(1,2,5)$ and $(1,2,4)$. Further they can both occur simultaneously. As can be seen in Figure 38, these embeddings are related by a Q-Twist hinged at $2,3,4,5$ and latched at 2 and 3.

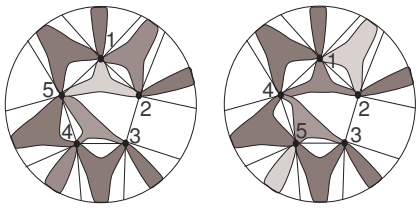

Figure 38.
$\sigma_{(12345)}$ and $\sigma_{(12354)}$ with patch $(3,4,5)$ - Related by a Q-Twist

In the second case, note that all four remaining patches can occur simultaneously as shown in Figure 39. The embeddings are related by a degenerate Q-Twist that moves the patch $(2,4,5)$ from the inside to the outside of the 5-cycle.

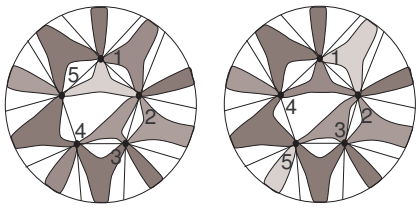

Figure 39.
$\sigma_{(12345)}$ and $\sigma_{(12354)}$ with no In-In Patch - Related by a Q-Twist

Case 2.3 By renumbering and reflecting around the vertical axis, we can assume that $\sigma_2 = \sigma_{(12453)}$. As before, we can assume that both Out-Out patches (i.e., $(1,3,4)$ and $(2,3,5)$) exist and are embedded on the outside of the 5-cycle. There are two possible In-In patches for σ_1 and σ_2: the $(1,2,3)$-patch and the $(3,4,5)$-patch: in Case 2.3.1, both of these patches exists; in Case 2.3.2, the $(1,2,3)$-patch exists and the $(3,4,5)$-patch does not; in Case 2.3.3, the $(1,2,3)$-patch does not exist and the $(3,4,5)$-patch does; and in Case 2.3.4, neither patch exists.

Case 2.3.1 Here none of the In-Out or Out-In patches can exist. This leads to the embeddings in Figure 40 which are related by a degenerate P-Twist. Consider the P-Twist in the Bowtie view from Figure 3. We obtain our desired degenerate P-Twist taking one embedding to the other as follows: Contract the patch labeled 1 to obtain node 1, contract the patch labeled 3 to obtain node 2, contract the two patches labeled 0 and 9 to obtain node 3, finally contract the edges on the patches labeled 2 and 4 that avoid the patches labeled 1 and 3 to obtain nodes 5 and 4 respectively.

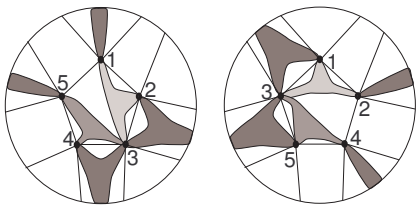

Figure 40.
$\sigma_{(12345)}$ and $\sigma_{(12453)}$ with both In-In Patches - Related By a P-Twist

Case 2.3.2 Here the only possible In-Out patch is $(1,4,5)$ and the only possible Out-In patch is $(2,4,5)$. Both can occur simultaneously. These two embeddings are shown in Figure 41. They are related by Q-Twists as follows. On the left embedding flip the $(1,3,4)$-patch, $(1,3)$-edge, and $(1,4)$-edge into the central pentagon. On the right embedding flip the $(2,3,5)$-patch, $(2,3)$-edge, and $(2,5)$-edge into the central pentagon. The resulting embeddings are the same because they both have the same central pentagon $(1,2,4,3,5)$ with no interior patches.

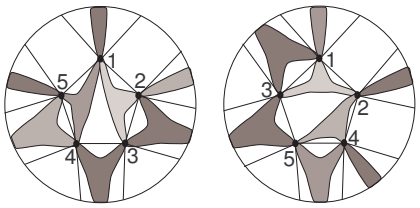

Figure 41.
$\sigma_{(12345)}$ and $\sigma_{(12453)}$ with five patches - Related by Q-Twists

Case 2.3.3 Here the only possible In-Out patch is $(1, 2, 5)$ and the only possible Out-In patch is $(1, 2, 4)$. Both can occur simultaneously. These two embeddings are related by a degenerate P-Twist as shown in Figure 42. Consider the P-Twist in the Bowtie view from Figure 3, then contract patches 1 and 2 to obtain vertex 2 and patch 9 to obtain vertex 5, contract the edge of patch 3 that avoids patch 8, the edge of patch 6 that avoids patch 2, and the edge of patch 0 that avoids patch 9.

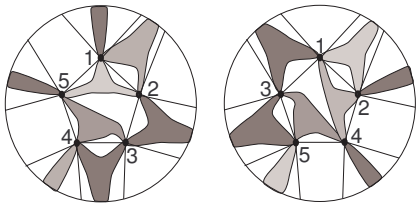

Figure 42.
$\sigma_{(12345)}$ and $\sigma_{(12453)}$ with five patches - Related by a P-Twist

Case 2.3.4 There are three In-Out patches and three Out-In patches to consider. It is clear that the maximal possible patch sets of In-Out patches are $\{(2, 3, 4), (4, 5, 1)\}$ and $\{(2, 3, 4), (1, 2, 5)\}$; similarly, the maximal possible patch sets of Out-In patches are $\{(1, 3, 5), (1, 2, 4)\}$ and $\{(1, 3, 5), (2, 4, 5)\}$. Furthermore, these maximal possibilities can occur simultaneously. This leads to four pairs of embeddings, each happen to be symmetric. One such pair is shown in Figure 43. They are related by a single Q-Twist hinged on 1,2,4,5 and latched on 1,4.

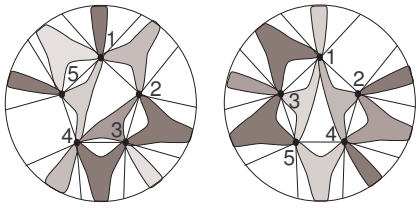

Figure 43.
$\sigma_{(12345)}$ and $\sigma_{(12453)}$ with no In-In Patches - Related by a Q-Twist

Case 2.4 By renumbering and reflecting around the vertical axis, we can assume that $\sigma_2 = \sigma_{(14253)}$.In this case, there are no Out-Out patches and no In-In patches possible. There are five possible In-Out patches $\{(1, 2, 3), (2, 3, 4), (3, 4, 5), (4, 5, 1), (5, 1, 2)\}$ and five possible Out-In patches $\{(1, 4, 2), (4, 2, 5), (2, 5, 3), (5, 3, 1), (3, 1, 4)\}$ for the pair of embeddings. Moreover, any patch from one set can embed simultaneously with any patch from the second.

So without loss of generality, we assume that $(1, 2, 3)$ exists in the patch structure. There are two possible In-Out patches that can also occur, $(3, 4, 5)$ and $(4, 5, 1)$. By symmetry, we can assume that $(3, 4, 5)$ occurs. Similarly, we consider the pairs of Out-In patches that occur. Up to symmetry and reversing σ_1 and σ_2, there are only two maximal structure that occurs: $(1, 2, 3), (3, 4, 5)$, $(2, 3, 5)$ and $(1, 2, 4)$ as shown in Figure 44, and $(1, 2, 3), (3, 4, 5)$, $(2, 3, 5)$ and $(1, 3, 4)$ as shown on the left in Figure

45. The first pair of patch embeddings are related by a P-Twist obtained from the Bowtie view in Figure 3, as follows: Contract patch 1 to obtain node 1, contract patch 3 to obtain node 2, contract patches 0 and 9 to obtain node 3, contact the edge of patch 4 that avoids patch 3 to obtain node 4, finally contract the edge of patch 2 that avoids patch 2 to obtain node 5. The patches $4, 5, 6$ and 7 remain. The leftmost patch embedding in Figure 45 is related to the rightmost embedding in the figure by flipping the $(1, 3)$- and $(3, 5)$-edges into the central pentagon. The reembedding from the middle embedding to the right embedding is the same reembedding as in Figure 40.

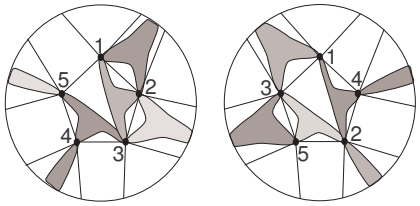

Figure 44.
$\sigma_{(12345)}$ and $\sigma_{(13524)}$ with patches $(1, 2, 3), (3, 4, 5)$, $(2, 3, 5)$ and $(1, 2, 4)$ - Related by a P-Twist

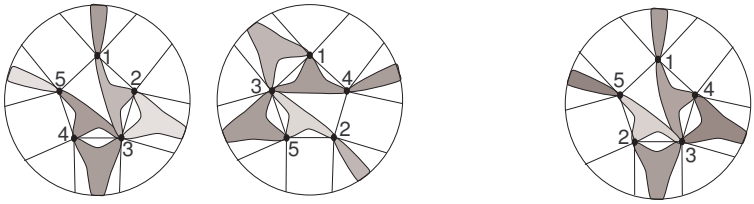

Figure 45.

$\sigma_{(12345)}$ and $\sigma_{(13524)}$ with patches $(1, 2, 3), (3, 4, 5)$, $(2, 3, 5)$ and $(1, 3, 4)$
Related by a Q-twist then a P-Twist

5.3.2 Frames that are subgraphs of double wheels

Let DW_n denote the double wheel graph with adjacent hub vertices whose rim has length n. Assume that F_G is isomorphic to an internally 4-connected subgraph of DW_n. Note that $DW_3 \cong K_5$, which was analyzed in Section 5.3.1. Hence we assume that $n \geq 4$. Assume that $v_1, v_2, \ldots, v_n$ are the vertices of the rim R in cyclic order and call the hub vertices a and b.

We assume that the projective plane is rendered as a disk with boundary covered by $\underline{v_1}, \ldots, \underline{v_n}, \overline{v_1}, \ldots, \overline{v_n}$ where $\underline{v_i} = \overline{v_i} = v_i$ but where the underlined vertices are along the top half of the disk and the overlined vertices are along the bottom half of the disk. In Figure 46 we show eight different embeddings of DW_n rendered in this way. Let ν_i be the embedding with two quadrangular faces on $\{v_i, v_{i-1}, a, b\}$. The embeddings ν_1 and ν_2 are shown in Figure 46. Let $\nu_{i,a}$ be the embedding obtained from ν_i by reembedding the av_i-spoke and define $\nu_{i,b}$ similarly: the embeddings $\nu_{n,a}$, $\nu_{n,b}$, $\nu_{1,a}$, $\nu_{1,b}$, $\nu_{2,a}$, and $\nu_{2,b}$ are also shown in Figure 46. If both av_i- and bv_i-spokes are reembedded, the resulting embedding is ν_{i+1}. One can show that there is no embedding of DW_n for $n \geq 4$ such that the rim cycle separates the projective plane and hence these $3n$ embeddings of DW_n are all the possible embeddings.

Deleting the ab-hub-edge or any rim edge from DW_n results in a planar graph. So for n even, the only internally 4-connected non-planar spanning subgraph G of DW_n is obtained by deleting spokes av_{2t-1} and bv_{2t} for all $1 \leq t \leq \frac{n}{2}$; call this subgraph AW_n. For n odd, there are no internally 4-connected non-planar subgraphs. Note that if $F_G \cong AW_4 \cong K_{3,3}$, then this case will be analyzed in Section 5.3.3. Hence for this section, we can assume that F_G is isomorphic to DW_n for $n \geq 4$ or AW_n for $n \geq 6$.

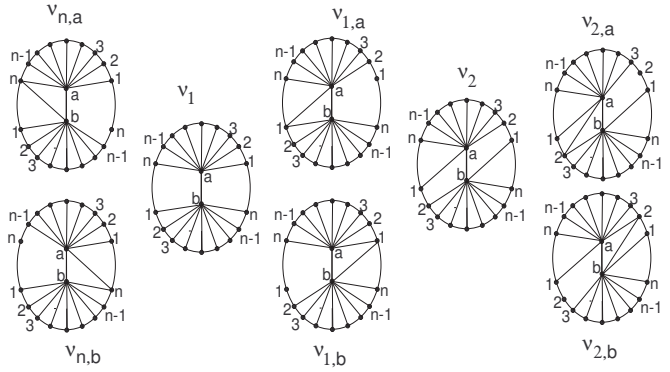

Figure 46. Some Reembedings of Double Wheels

In this and subsequent sections, we will often show that a certain patch structure on a frame graph F_G will give rise to a subdivision of V_8 in the graph G. In these cases, we can refer back to the proof in Section 4 to complete the proof.

First, suppose σ_1 and σ_2 are two patch embeddings of $F_G = AW_m$ for $m \geq 6$. Note that for any embedding of AW_n with $n \geq 6$ the rim R must be non-contractible. Furthermore, $\nu_{i,a}$ restricted to AW_n is the same as ν_{i+1} restricted to AW_n. Thus the only embeddings of AW_n are $\nu_1, \ldots, \nu_n$ restricted to AW_n. Also since AW_n has no triangles, it has no patches. So if $\sigma_1 = \nu_j$ and $\sigma_2 = \nu_k$, we can take σ_1 to σ_2 by a sequence of degenerate Q-Twists that move one spoke of the wheel at a time.

Now suppose σ_1 and σ_2 are two patch embeddings of $F_G = DW_n$ for $n \geq 4$. There are two types of patches possible in these embeddings of DW_n, *hub patches* on (a, b, v_j) and *rim patches* on (a, v_j, v_{j+1}) or (b, v_j, v_{j+1}). In Case 1 say that $n \geq 5$ and in Case 2 say that $n = 4$.

Case 1 Label the rim vertices of DW_5 by 1,2,3,4,5 and the hub vertices by 6,7. If we perform a ΔY operation on triangle $1, 6, 7$ and then delete edges $(2, 6), (4, 6), (3, 7), (5, 7)$ we obtain V_8. Thus any hub patch on $F_G \cong DW_n$ implies that G has a V_8-minor and so we assume there are no hub patches on F_G. Also if we double the $(1, 2)$-edge and then perform ΔY operations on triangles 1,2,6 and 1,2,7, then we can contract the $(2, 3)$-edge and delete edges $(3, 6), (4, 6), (3, 7), (5, 7)$ we obtain V_8. Thus any two rim patches (a, v_j, v_{j+1}) and (b, v_j, v_{j+1}) on F_G will imply that G has a V_8-minor and so we assume that there are no two such patches. In Case 1.1 say that there is a double rim patch and in Case 1.2 say there is no double rim patch.

Case 1.1 In Figure 47, we show all of the patch embeddings of DW_n with a double rim patch on (v_1, v_n, a) up to exchanging of the two patches. Other patches may be present but they are fixed pointwise with respect to our renderings. These embeddings are all related by degenerate Q-Twists that move a single edge or interchange the patches.

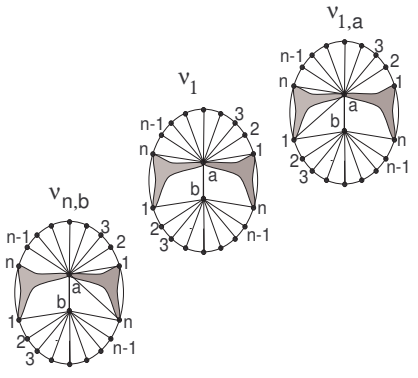

Figure 47.

Case 1.2 Here for each rim edge (v_{j-1}, v_j) either there is no rim patch on (v_{j-1}, v_j), a single (v_{j-1}, v_j, a)-patch, a single (v_{j-1}, v_j, b)-patch, but not both rim patches. As shown in Figure 47, a (v_{j-1}, v_j, a)-patch is fixed pointwise in our rendered embeddings of DW_n save in $\nu_{j-1,b}$, ν_j, and $\nu_{j,a}$. In a given embedding of DW_n, two rim patches with nonadjacent rim edges cannot both be flexible. Similarly, two rim patches with adjacent rim edges and the same hub vertex cannot both be flexible. Two rim patches with adjacent edges and different hub vertices are both flexible in a single embedding of DW_n. Figure 48 shows all of the possible patch embeddings for DW_n with a (v_n, v_1, a)-patch and (v_1, v_2, b)-patch in the five embeddings of DW_n in which one or both patches are flexible.

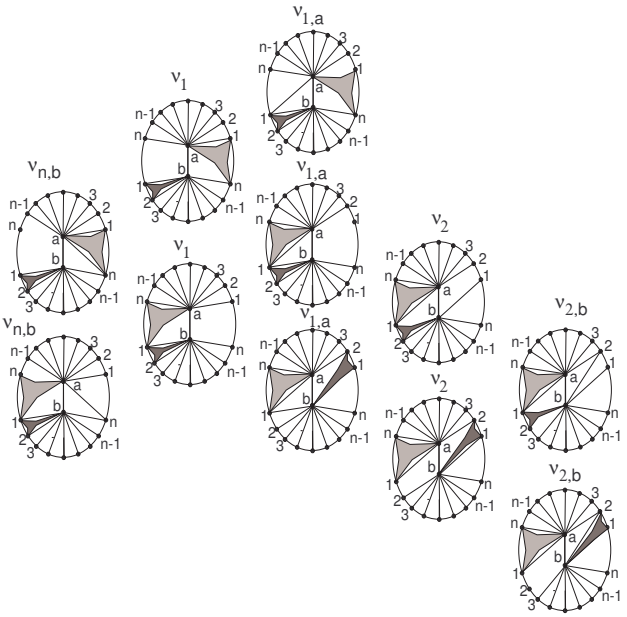

Figure 48.

So we see that any patch embedding of DW_n without two patches on the same rim edge may use any embedding of the frame DW_n. When any single patch or any single edge of DW_n is flexibile, they may be reembedded individually by Q-Twists in a certain order. When multiple rim patches and single edges are flexible, the possible embeddings are shown in Figure 48 where again we see that we may always reembed patches and edges individually to get from one embedding to another.

Case 2 First we give some patch configurations on DW_4 that produce a V_8-minor in G. For this discussion label the rim vertices of DW_4 with 1,2,3,4 and hub vertices with a,b.

First, any hub patch and rim patch together create a V_8-minor. To see this perform ΔY-operations on triangles $(1, 2, a)$ and $(4, a, b)$ and delete the $(3, b)$-edge to obtain V_8. Next perform ΔY-operations on triangles $(1, 2, a)$ and $(1, a, b)$ and delete the $(4, a)$- and $(3, b)$-edges to obtain V_8.

Second, any two hub patches with adjacent rim vertices together create a V_8-minor. To see this perform ΔY-operations on the triangles $(1, a, b)$ and $(2, a, b)$ and delete the $(3, a)$- and $(4, b)$-edges to obtain V_8. Note also that it is not possible at all to embed two hub patches with nonadjacent rim vertices.

So now the only possible patch configurations that do not produce a V_8-minor in G are a single or double hub patch or solely rim patches. In the latter case, we obtain the result that any two patch embeddings are related by Q-Twists as in Case 1. In the former case, we show all possible patch embeddings of DW_4 with a single hub patch, say $(1, a, b)$ in Figure 49. In some of the embeddings it is possible to have a double hub patch. One can see that these embeddings are all related by Q-Twists.

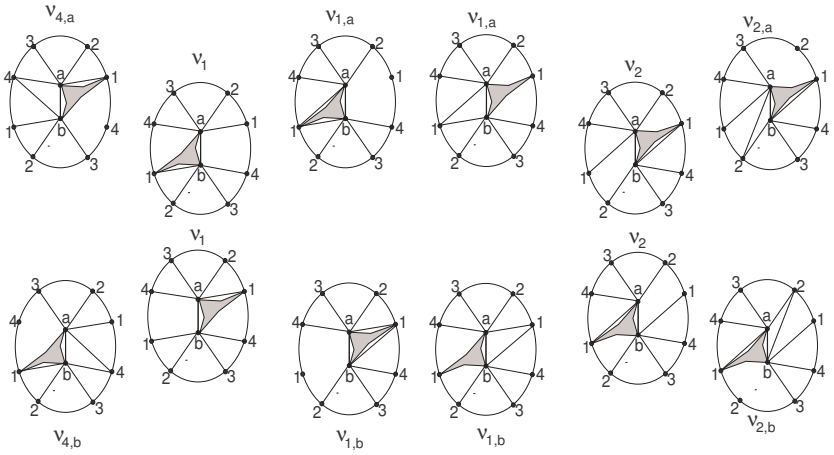

Figure 49.

5.3.3 Frames on six vertices

In each of Sections 5.3.3–5.3.8, we will use the following naming conventions for the many graphs needed in the analysis. Given two graphs G and H, GH will denote the disjoint union while $\overline{G}$ will denote the complement of G. For k a positive integer, C_k will be the cycle on k edges, P_k will be the path on k edges, M_k will be the matching graph on k edges, K_k will be the complete graph on k vertices and E_k will be the edgeless graph on k vertices. Let N_4 be a 3-pan graph, i.e. a triangle with a pendant edge. Let B_7, the bowtie graph, be obtained by identifying the vertices of degree one in two copies of N_4.

There are four internally 4-connected nonplanar graphs on six vertices: K_6, $K_6\backslash e$, DW_4, and $K_{3,3}$. We have analyzed the case where $F_G \cong DW_4$ in Section 5.3.2 on double wheels. In the case that $F_G \cong K_{3,3}$, there are no patches because $K_{3,3}$ has no triangles. There are six embeddings of $K_{3,3}$ and they are shown in Figure 25 and they are all related by Q-Twists. So we need only analyze the cases for K_6 and $K_6\backslash e$. Let these be Cases 1 and 2, respectively.

Case 1 There is a unique unlabeled projective-planar embedding of K_6, which is a triangulation. If there are no patches on the frame, then there are twelve distinct embeddings. To see this consider the vertex 0 fixed in the center of a 5-cycle. Vitray [19, Thm.5.2.3] showed that a Q-twist on such an embedding has the effect of transposing two vertices on the 5-cycle. Hence, any embedding of K_6 with no patches can be obtained from any other embedding by a sequence of Q-Twists. Note that a given patch might not be allowable in one of the intermediate embeddings in the sequence.

To analyze the possible patch structures, label the vertices $0, 1, 2, 3, 4, 5$. In Figure 50 we show the six possible labeled embeddings where $0, 1, 5$ is a facial triangle and $4, 5, 6$ is a noncontractible cycle. The remaining six embeddings of K_6 have $4, 5, 6$ as a facial triangle and $0, 1, 5$ as a noncontractible cycle.

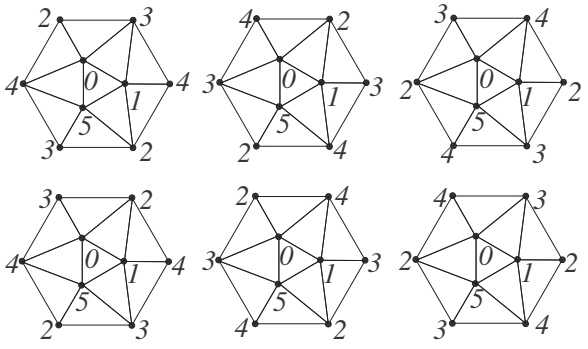

Figure 50.

Without loss of generality assume there is a $(0, 1, 5)$-patch. So we can assume that each of σ_1 and σ_2 is one of the embeddings shown in Figure 50. Since K_6 is 3-representative in the projective plane, any

patch must be embedded within the triangular face of its three vertices of attachment and there can be no double patches. This implies that any two patch embeddings of K_6 with the same underlying embedding of K_6 and the same set of patches are the same patch embeddings. So without loss of generality assume we have patch embedding σ_1 with K_6 as shown in the upper left of Figure 50. Up to symmetry there are two types of frame embeddings possible for σ_2, one with a transposition on the boundary and one with a rotation on the boundary. These two patch embeddings are shown in with the maximal patch structures in Figure 51.

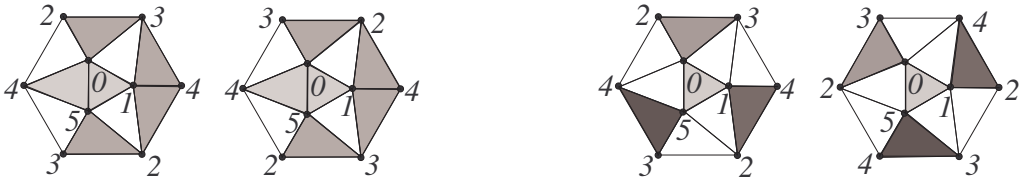

Figure 51.

The reembedding on the left is a Q-Twist hinged at $0, 2, 3, 5$ and latched at $1, 4$ (and then reflected along a horizontal line). The reembedding on the right is a degenerate P-Twist obtained from the central view of the P-Twist (see Figure 3) by contracting patches 6 and 2 to an edge, patches 3 and 8 to an edge, and patches 5 and 9 to an edge.

Case 2 Suppose $F_G \cong K_6\backslash e$, K_6 with the edge $(1, 2)$ removed. There are two types of embeddings of this graph: those that extend to an embedding of K_6 and those that do not. There are twelve embeddings of the first type and six of the latter type which are shown in Figure 52. In each of these six embeddings the embedding of the K_4 induced on $\{3, 4, 5, 6\}$ can be assumed to be fixed.

Figure 52.

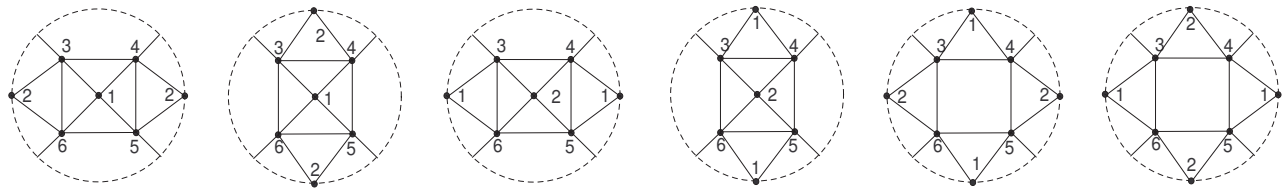

Six of the eighteen embeddings of $K_6\backslash e$

Given any patch embedding of $F_G = K_6\backslash e$, if the frame is embedded in an extendable fashion, then the quadrilateral face of F_G bounded by vertices $1, u, 2, v$ cannot have a $(1, 2, u)$- or $(1, 2, v)$-patch because these are not triangles in F_G. Thus we can flip the (u, v)-edge into the quadrilateral and so F_G is now embedded in a nonextendable fashion. Therefore we can assume that we have patch embeddings σ_1 and σ_2 with the embeddings of F_G as in Figure 52. After relabeling, we can assume that σ_1 is the leftmost embedding in Figure 52. Up to symmetry there are four possibilities for σ_2: the first, the third, the fourth, or the fifth embedding in the Figure. Let these be Cases 2.1–2.4, respectively. In each case notice that there are exactly two 2-representative cuts in each of the embeddings of F_G and no cut can be moved off a vertex onto an incident edge. Thus the placement of patches is uniquely determined in each embedding of F_G.

Case 2.1 Here we must have $\sigma_1 = \sigma_2$ as any patch has a unique position up to isotopy.

Case 2.2 Here the only possible patches incident to vertices 1 or 2 are: $(2, 3, 6)$, $(1, 3, 6)$, $(1, 4, 5)$, and $(2, 4, 5)$. There may also be patches on $3, 4, 5, 6$ as well but these are exterior to the quadrilateral on $3, 4, 5, 6$ and so we can go from σ_1 to σ_2 by a single Q-Twist hinged at $3, 4, 5, 6$ and latched at 1 and 2.

Case 2.3 Up to symmetry the maximal configuration of patches possible is shown in Figure 53. We can go from the first embedding to the second by two Q-Twists. The first hinged on $3, 4, 5, 6$ and latched on $1, 6$ and the second hinged on $3, 4, 5, 6$ and latched on $2, 4$.

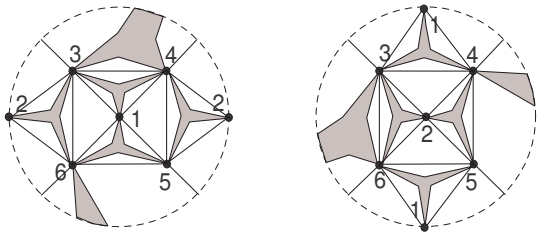

Figure 53.

Case 2.4 The intermediate patch embedding in Case 2.3 has up to symmetry the maximal possible configuration of patches and so we go between the two embeddings by the first Q-Twist in Case 2.3.

5.3.4 Frames on seven vertices

In this section, we assume that G has a frame graph F_G which has seven vertices.

Proposition 5.6. *There are exactly 28 internally* 4*-connected graphs on seven vertices. Of these graphs, one is planar and seven are non-projective planar.*

Proof. Let G be an internally-4-connected graph on seven vertices. If $\delta(G) = 6$, then G must be isomorphic to K_7. If $\delta(G) = 5$, then $\Delta(\overline{G}) = 1$. Hence G is isomorphic to either $\overline{M_1E_5}$, $\overline{M_2E_3}$ or $\overline{M_3E_1}$, which are all internally 4-connected. In the case when $\delta(G) = 4$, as $\overline{C_4E_3}, \overline{C_4M_1E_1}, \overline{C_4P_2}$ and $\overline{C_4C_3}$ are not internally-4-connected, G must be one of the following 21 graphs: $\overline{C_3E_4}$, $\overline{C_5E_2}$, $\overline{C_6E_1}$, $\overline{C_7}$, $\overline{P_2E_4}$, $\overline{P_3E_3}$, $\overline{P_4E_2}$, $\overline{P_5E_1}$, $\overline{P_6}$, $\overline{C_3C_3E_1}$, $\overline{P_2P_2E_1}$, $\overline{P_2P_3}$, $\overline{C_3P_2E_1}$, $\overline{C_3P_3}$, $\overline{C_3M_1E_2}$, $\overline{C_3M_2}$, $\overline{C_5M_1}$, $\overline{P_2M_1E_2}$, $\overline{P_2M_2}$, $\overline{P_3M_1E_1}$, and $\overline{P_4M_1}$.

Finally, in the case $\delta(G) = 3$, let v be a 3-valent vertex and label the neighbors of v as v_1, v_2, v_3 and the remaining three vertices as v_a, v_b, v_c. By internal 4-connectivity, v_1, v_2, v_3 are independent. Vertex v_1 must then be adjacent to at least two of v_1, v_b, v_c. If v_1 is only adjacent to v_a and v_b, then by internal 4-connectivity v_a and v_b are nonadjacent. In order to excluded 3-separations with five vertices on each side we now must have that v_c is adjacent to both v_a and v_b and v_2 and v_4 are both adjacent to all of v_a, v_b, v_c. Thus $G = \overline{B_7}$. If v_1 has degree 4, then without loss of generality v_2 and v_3 both have degree 4 and since $K_{3,4}$ is not internally 4-connected we now get that $G = \overline{C_3K_{1,3}}$ or $G = \overline{C_3N_4}$.

Note that $\overline{C_5M_1}$ is a planar double wheel. Further, $\overline{M_3E_1}$ and $\overline{P_4E_2}$ are isomorphic to A_2 and B_1 respectively in Archdeacon's list of 35 minor-minimal non-projective-planar graphs (see, e.g., [9]). Hence, $\overline{M_3E_1}$, $\overline{P_4E_2}$, $\overline{M_2E_3}$, $\overline{M_1E_5}$, $\overline{P_3E_3}$, $\overline{P_2E_4}$ and K_7 are all not projective-planar. □

Hence we need to consider the flexibility of graphs G whose frame F_G is isomorphic to one of the graphs in the set $\mathcal{L}$ which consists of the 20 internally 4-connected projective planar, non-planar graphs listed in the proof of Proposition 5.6. We will analyze these graphs according to whether they contain a $K_{3,4}$-subgraph, a $\overline{C_7}$-subgraph, or neither.

There are 13 graphs in $\mathcal{L}$ that contain a $K_{3,4}$-subgraph: $\overline{C_3E_4}$, $\overline{P_2M_1E_2}$, $\overline{C_3M_1E_2}$, $\overline{P_3M_1E_1}$, $\overline{P_2P_2E_1}$, $\overline{P_2M_2}$, $\overline{C_3P_2E_1}$, $\overline{C_3M_2}$, $\overline{P_2P_3}$, $\overline{C_3C_3E_1}$, $\overline{C_3P_3}$, $\overline{C_3K_{1,3}}$ and $\overline{C_3N_4}$. These 13 graphs will be analyzed in Section 5.3.5

There are four graphs in $\mathcal{L}$ that do not contain a $K_{3,4}$-subgraph but contain a $\overline{C_7}$: $\overline{C_7}, \overline{P_6}, \overline{P_5E_1}$, and $\overline{P_4M_1}$. These four graphs will be analyzed in Section 5.3.6.

There are three remaining graphs in $\mathcal{L}$: $\overline{C_6E_1}, \overline{C_5E_2}$ and $\overline{B_7}$. These three graphs will be analyzed in Section 5.3.7.

5.3.5 Frames that contain a $K_{3,4}$ subgraph

First, we consider the case when F_G is isomorphic to one of the 13 graphs in $\mathcal{L}$ that contain a $K_{3,4}$-subgraph. The six embeddings of $K_{3,4}$ are shown on the left of Figure 54 where the arrows represent relation by a single Q-Twist. Label the vertices of the two partite sets of the $K_{3,4}$-subgraph are $\{1,2,3\}$ and $\{4,5,6,7\}$. In Case 1, we will consider the case when vertices $1,2,3$ are independent. In Case 2, we will consider the case when there is at least one edge in $\{1,2,3\}$.

Case 1 Here $K_{3,4} \subseteq F_G \subseteq \overline{C_3E_4}$. Each of the six embeddings of $K_{3,4}$ extend uniquely to an embedding of $\overline{C_3E_4}$. These embeddings are shown on the right of Figure 54. The only 2-representative cuts of an embedding of $K_{3,4}$ pass through two of the vertices $\{1,2,3\}$. In particular, there are no 2-representative cuts that pass through the interior of an edge. As such any patch on F_G has a unique placement in any embedding of F_G.

Any two embeddings of F_G are related by either a single Q-Twist or a single P-Twist. The arrows in Figure 54 represent Q-Twists similar to the one show on the top right of the figure for $\overline{C_3E_4}$ latched at $\{4,6\}$ and hinged at $\{2,3,5,7\}$ which transpose the vertices in 2 and 3. Any patches on F_G common to both of these embeddings are preserved by this Q-Twist. For two embeddings not connected by an arrow (without loss of generality take the top embedding and the lower left embedding) there is a degenerate P-Twist that will reembed the graph $\overline{C_3E_4}$ with a rotation on vertices $\{1,2,3\}$. This can be seen by contracting patches $0,1,4,7$ in the central view of the P-Twist structure shown in Figure 3. Note that all patches that embed in both frame embeddings obey the P-Twist. See Figure 55.

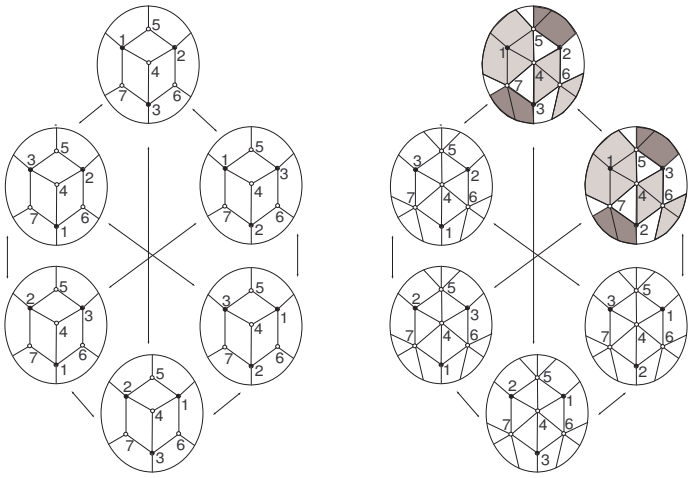

Figure 54. Flexibility of $K_{3,4}$ and $\overline{C_3E_4}$ by Q-Twists

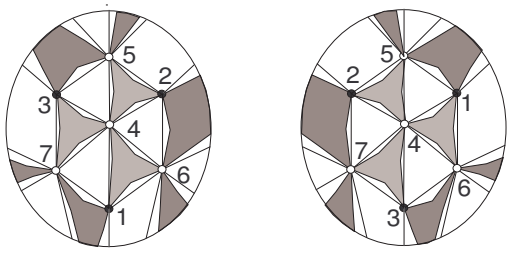

Figure 55. Rotations of $\{1,2,3\}$ in $\overline{C_3E_4}$ by Degenerate P-Twist

Case 2 Of the 13 graphs contained in $\mathcal{L}$ that contain a $K_{3,4}$-subgraph, it remains to consider the case when F_G is isomorphic to one of those graphs that contain at least one edge on the vertices $\{1,2,3\}$.

These are the five graphs: $\overline{P_2M_1E_2}$, $\overline{P_3M_1E_1}$, $\overline{P_2P_2E_1}$, $\overline{P_2P_3}$ and $\overline{P_2M_2}$. These will be Cases 2.1–2.5 respectively.

Case 2.1 We may assume that there is an edge $\{1,2\}$ in F_G. As before, all of the edges on $\{4,5,6,7\}$ are uniquely embeddable in each of the six embeddings of $K_{3,4}$. By symmetry, we may assume that $(4,5)$ is the missing edge on $\{4,5,6,7\}$. However, once the remaining five edges are in place, the edge $(1,2)$ can only be embedded in two of the six cases (See Figure 56). These two embeddings with all of their possible common patches are related by a Q-Twist hinged as shown in Figure 56.

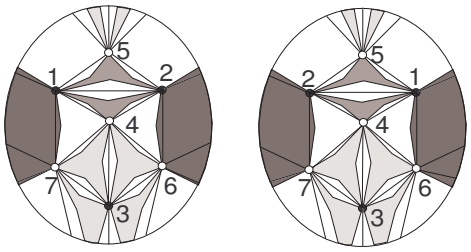

Figure 56.
Flexibility of $\overline{P_2M_1E_2}$ by Q-Twists

Case 2.2 We can assume that the missing edges are $(1,3)$ and the path $\{6,4,7,5\}$. Again, the three remaining edges on $\{4,5,6,7\}$ are uniquely embeddable in each of the six embeddings of $K_{3,4}$. After these edges are in place, the edges $(1,2)$ and $(2,3)$ only embed in two of the six possible cases. However, in both cases, one of the edges can embed in two distinct ways. See Figure 57 for these four embeddings along with all of the possible common patches. The flexible edges are shown as dotted lines in both positions. These embeddings are related by a single Q-Twist hinged at $1,2,3,6$ and latched at $2,5$ and by reembeddings of the single edges as shown.

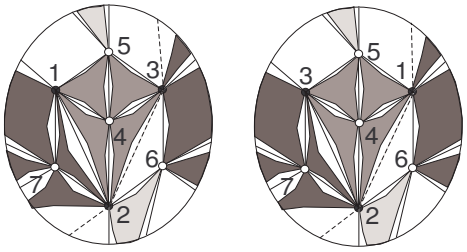

Figure 57.
Flexibility of $\overline{P_3M_1E_1}$ by Q-Twists

Case 2.3 We can assume that the missing paths are $\{2,1,3\}$ and $\{5,4,6\}$. Again, the four edges on $\{4,5,6,7\}$ are uniquely embeddable in each of the six embeddings of $K_{3,4}$. In this graph, the edge $(2,3)$ is not embeddable in two of the six embeddings, while in the remaining four, it belongs to a unique face. Hence there are exactly four embeddings of $\overline{P_2P_2E_1}$ as shown on the left in Figure 58. The arrows between embeddings in Figure 58 indicate Q-Twist operations relating the two embeddings. All possible patches in common to the two embeddings in the top row are shown to respect the Q-Twist. The maximal sets of patches for the pairs of embeddings in the other three cases also obey the respective Q-Twists similarly. All possible common patches for the upper left and lower right embeddings are shown in the rightmost column of Figure 58. These two patch embeddings are related by a degenerate P-Twist as follows. Take the bowtie view of the P-Twist and contract patches 2,5,8 and contract an edge of 7 and 0 to as shown in the three columns on the right in Figure . The P-Twist operation to relate the patch structures on the lower left and upper right embeddings is similar. Note that these embeddings are not related by a Q-Twist as there are seven vertices whose cyclic ordering of their neighbors is changed, while a Q-Twist only allows for at most six such vertices.

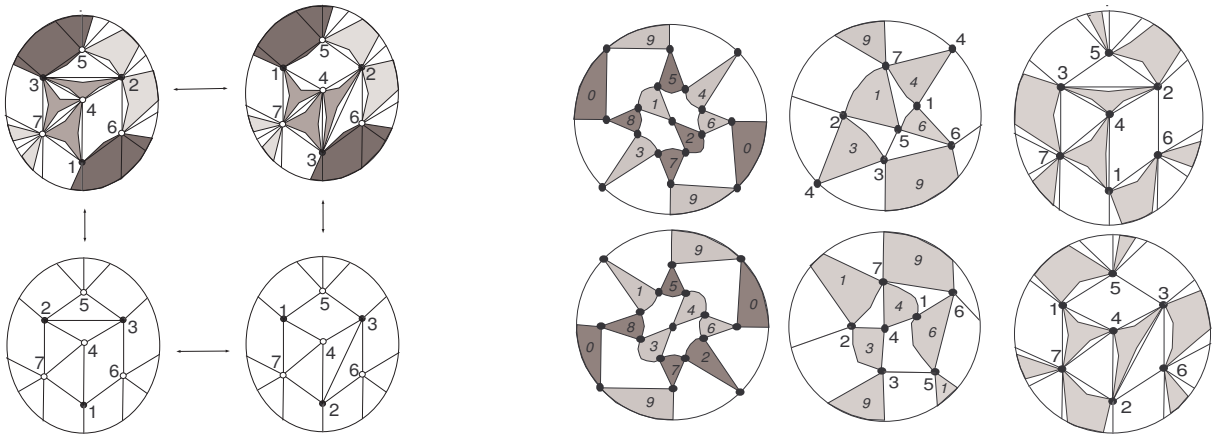

Figure 58.

Case 2.4 This graph is isomorphic to $\overline{P_2P_2E_1}$ with the edge $(5,7)$ deleted. The only embeddings in addition to the ones in Case 2.3 are shown in Figure 59 where the $(2,3)$-edge can be reembedded as shown. So now any two patch embeddings are related as they are in Case 2.3 after possible reembedding of the $(2,3)$-edge.

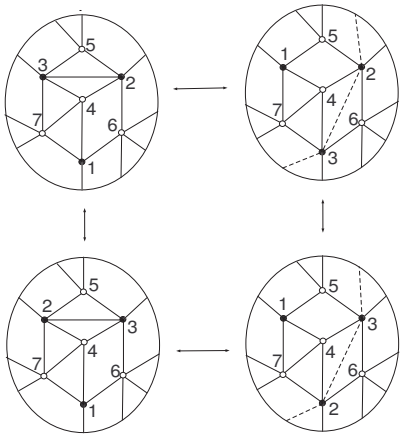

Figure 59.
Flexibility of $\overline{P_2P_3}$ by Q-Twists

Case 2.5 We can assume that the missing path is $\{2,1,3\}$ and the missing matching is $(4,5)$ and $(6,7)$. Again, the four edges on $\{4,5,6,7\}$ are uniquely embeddable in each of the six embeddings of $K_{3,4}$. In this case, the edge $(2,3)$ is not embeddable in four of the six embeddings of $K_{3,4}$, while in the remaining two, the edge can belong to two faces in each embedding. Hence there are four embeddings of $\overline{P_2M_2}$ as shown in Figure 60 with the flexible $(2,3)$-edge as indicated. Regardless of the position of the $(2,3)$-edge, the possible common patches shown in Figure 60 follow the Q-Twist indicated by the shading of the patches.

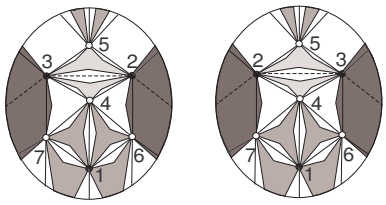

Figure 60.
Flexibility of $\overline{P_2M_2}$ by Q-Twists

5.3.6 Frames that contain $\overline{C_7}$

Now we will consider the flexibility of the graphs in $\mathcal{L}$ that contain a $\overline{C_7}$-subgraph, but no $K_{3,4}$-subgraph. There are four such graphs, $\overline{C_7}, \overline{P_6}, \overline{P_5E_1}$, and $\overline{P_4M_1}$. Consider these to be Cases 1–4, respectively. See Figure 61.

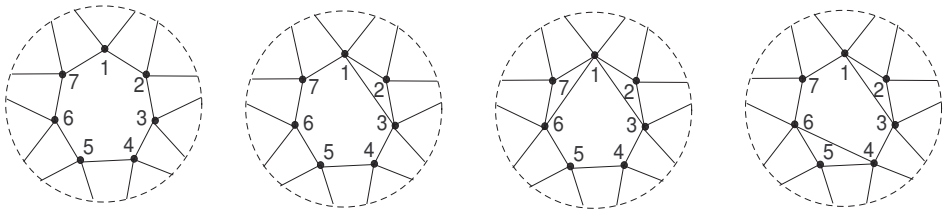

Figure 61. Graphs $\overline{C_7}, \overline{P_6}, \overline{P_5E_1}$, and $\overline{P_4M_1}$

Case 1 The graph $\overline{C_7}$ has 15 embeddings on the projective plane. To describe them, let the vertices of the seven cycle be $\{1, 2, 3, 4, 5, 6, 7\}$, the remaining edges are $(i, i+4)$ for $1 \leq i \leq 7 \pmod 7$. It is straightforward to verify that in any embedding the seven cycle must be contractible. Further, at most two of the non-cycle edges can belong to the interior of the 7-cycle in any embedding. Moreover, if there are two non-cycle edges in the 7-face, they must share a common endpoint. Hence the embeddings fall into three types: the standard embedding with all non-cycle edges in the outside of the cycle; the seven embeddings with a single non-cycle edge inside the 7-cycle; the seven embeddings with both non-cycle edges incident with vertex i inside the 7-cycle. Recall that moving a single edge from the inside of the 7-cycle to the outside of the cycle is a degenerate Q-Twist and so any two embeddings of $\overline{C_7}$ are related by Q-Twists. This completes Case 1 because any one patch on $F_G \cong \overline{C_7}$, creates a V_8-minor in G. This can be seen as follows. Up to symmetry we may assume there is a patch on $\{1, 4, 5\}$ and so G contains a minor equal to the graph obtained from $\overline{C_7}$ by a ΔY-operation on the triangle $\{1, 4, 5\}$. By inspection one can find a V_8-subgraph.

Case 2 Consider the graph $\overline{P_6}$. We can assume that this graph is obtained from $\overline{C_7}$ as described above by adding the edge $(1, 3)$. Any embedding of this graph contains an embedding of $\overline{C_7}$. In none of the 15 embeddings of $\overline{C_7}$ is it possible to add the edge $(1, 3)$ to the outside of the 7-cycle. It can also be checked that in 10 of the 15 embeddings of $\overline{C_7}$ the edge $(1, 3)$ can be included inside the 7-cycle. Moreover, any two of these embeddings are related by moving single edges in and out of the 7-cycle in succession.

As in Case 1, if there were a patch attached to a triangle of $\overline{C_7}$, then G would contain a V_8-minor. Hence we need only consider triangles that contain the new edge, $(1, 3)$. There are two such triangles $(1, 3, 4)$ and $(1, 3, 7)$. One can check that a ΔY-operation on either triangle also leads to a V_8-subgraph in G.

Case 3 Consider the graph $\overline{P_5E_1}$. We can assume that this graph is obtained from $\overline{C_7}$ by adding the edges $(1, 3)$ and $(1, 6)$. Both of these edges must be embedded inside the 7-cycle in each embedding. Only edges that are not skew to either $(1, 3)$ or $(1, 6)$ on the 7-cycle can be moved to the inside of the 7-cycle. This allows only five embeddings of $\overline{P_5E_1}$: the embedding shown in Figure 61, the embedding with $(3, 6)$-edge flipped in, the embedding with $(1, 4)$-edge flipped in, the embedding with $(1, 5)$-edge in and the embedding with both $(1, 4)$- and $(1, 5)$-edge flipped in. Again these embeddings are all related by Q-Twists.

As in Case 2, if there is any patch on F_G other than the $(1, 3, 6)$-patch, then there is a V_8-minor in G. The $(1, 3, 6)$-patch, however, can only be placed in the embedding of $\overline{P_5E_1}$ that is shown in Figure 61 and the embedding of $\overline{P_5E_1}$ with the $(3, 6)$-edge flipped into the 7-cycle. This pair of patch embeddings is related by flipping an edge.

Case 4 We can assume that this graph is obtained from $\overline{C_7}$ by adding the edges $(1,3)$ and $(4,6)$. Again, both of these edges must be inside the 7-cycle in each embedding. Only edges that are not skew to either $(1,3)$ or $(4,6)$ can be moved to the inside of the 7-cycle. This allows only eight embeddings of $\overline{P_4M_1}$. When there are no patches, these embeddings are related by Q-Twists. Similar to in Case 2, any patch would create a V_8-minor in G.

5.3.7 Frame isomorphic to remaining three graphs on seven vertices

There are only three more graphs in $\mathcal{L}$ to consider. They are $\overline{C_5E_2}$, $\overline{C_6E_1}$ and $\overline{B_7}$. The graph $\overline{C_5E_2}$ is a double wheel graph and was considered in Section 5.3.2.

Frames isomorphic to $\overline{C_6E_1}$ The graph $\overline{C_6E_1}$ consists of a 3-prism plus a seventh vertex adjacent to each of those in the prism. If we label the two triangles of the prism as 1,2,3 and 4,5,6, then one can check that both triangles must be embedded contractibly. Furthermore, the prism cannot be embedded in a disk and so all possible embeddings of $\overline{C_6E_1}$ are shown in Figure 62 where the dashed lines represent edges with flexibilities. This makes a total of twelve different embeddings.

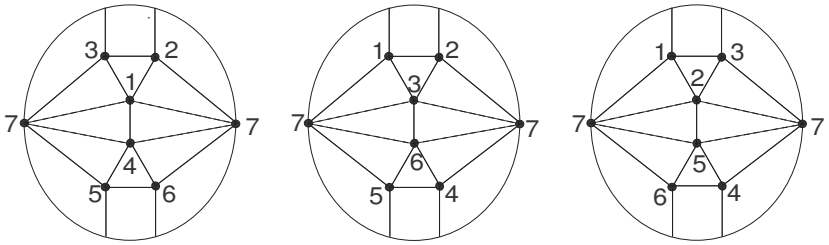

Figure 62.

Let σ_1 and σ_2 be two different embeddings of G with $F_G \cong \overline{C_6E_1}$. Without loss of generality assume that $\sigma_1|_{F_G}$ is shown on the left in Figure 62. There are three possibilities for $\sigma_2|_{F_G}$.

If $\sigma_2|_{F_G}$ is also as shown on the left in the figure, then only a $(1,4,7)$-patch on F_G can be embedded in more than one place. This would be the only difference between σ_1 and σ_2 aside from the flexible $(1,7)$- and $(1,4)$-edges. Thus we can go from σ_1 to σ_2 by at most three Q-Twists.

If $\sigma_2|_{F_G}$ is also as shown in the middle in the figure, the patches common to both embeddings of F_G are shown in Figure 63. As long as the flexible edges incident to vertex 7 are embedded as shown in Figure 63, then we can go between the embeddings shown in this figure by a degenerate Q-Twist whose three patches are given the three different shades in Figure 63. The flexible edges incident to vertex 7 can be, of course, reembedded by Q-Twists. The case were $\sigma_2|_{F_G}$ is also as shown on the right in the figure is resolved with a similar Q-Twist.

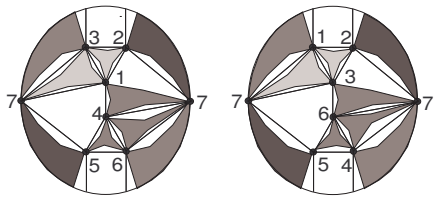

Figure 63.

Frame isomorphic to $\overline{B_7}$ Consider the case when the frame graph F_G is isomorphic to $\overline{B_7}$. Let the $K_{3,3}$ subgraph of $\overline{B_7}$ have partite sets $\{1,2,3\}$ and $\{5,6,7\}$ and let the remaining vertex be adjacent to $\{2,3,6,7\}$. The $K_{3,3}$ subgraph can be embedded in exactly six ways. The final vertex 4 can then be embedded in a unique face in four of those embeddings and in one of two faces in the remaining two embeddings. Thus Figure 64 shows all embeddings of $\overline{B_7}$.

Notice that there are only four triangles in $\overline{B_7}$ and hence only four possible patches: $(4,2,6)$, $(4,6,3)$, $(4,3,7)$, and $(4,7,2)$. Furthermore, no patch can embed in more then one place in any of the eight embeddings of $\overline{B_7}$. Thus if two embeddings of G have the frame F_G embedded in the same way, then the two embeddings of G are the same.

Now in each of the embeddings labeled A, B, C, D, E, or F, all four patches can embed simultaneously as shown in Figure 65. It is straightforward to check that those pairs of embeddings with arrows connecting them are related by degenerate Q-Twists. For example, embedding A can be taken to embedding B by a Q-Twist hinged at $5,3,2,7$ and latched at $1,7$. In this case, we do not need to worry about the pairs of embeddings at distance two, since all possible patches obey the intermediate embedding, we can simply use two Q-Twists.

In embedding H, only two patches are possible, $(4,2,6)$ and $(4,3,7)$. It is clear that a Q-Twist will take that patch embedding to the patch embedding corresponding to embedding F. That embedding is then related to any other patch embedding with those two patches as above. The case of embedding G is symmetric. If the two embeddings of the frame correspond to embeddings H and G, then there can be no patches and they are related by a Q-Twist.

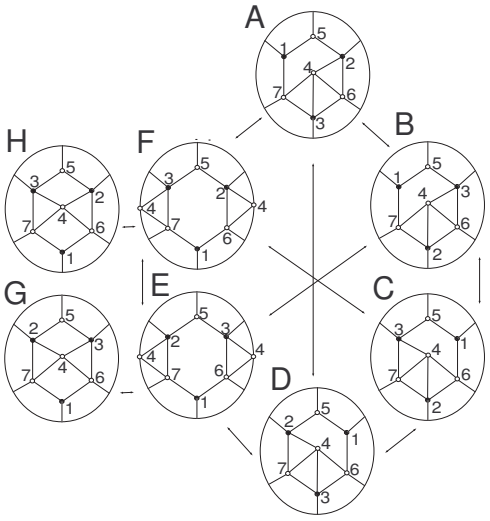

Figure 64.
Eight Embeddings of $\overline{B_7}$

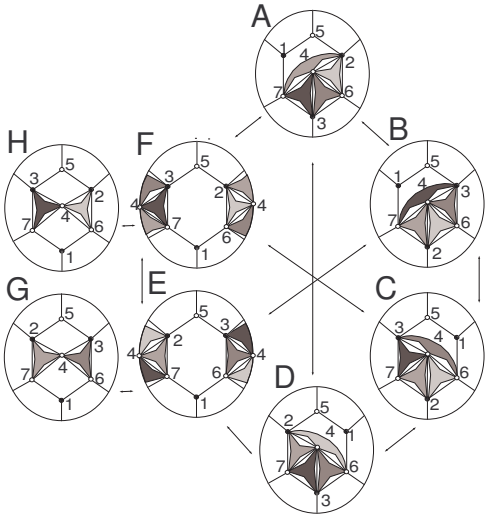

Figure 65.
Patch Embeddings of $\overline{B_7}$

5.3.8 Frames that are 4-vertex coverable graphs

Suppose F_G is a 4-vertex coverable graph on at least 8 vertices. Hence there exist four vertices $a, b, c, d \in V(F_G)$ such that $V(F_G) \setminus \{a, b, c, d\} = \{v_1, v_2, v_3, \ldots, v_t\}$ is independent. Note that $t \geq 4$ and all of the vertices v_i must have exactly three or four neighbors in $\{a, b, c, d\}$. Let $v_1, \ldots, v_m$ have degree four, while $v_{m+1}, \ldots, v_t$ have degree three in G. Note that, as $K_{4,4}$ cannot be embedded in the projective plane, $m \leq 3$. Also note that if two vertices in $v_{m+1}, \ldots, v_t$ have the same three neighbors, those vertices would violate internal-4-connectivity and so $n = t - m \leq 4$.

Suppose $m = 3$ and $n \in \{1, 2, 3, 4\}$, then F_G contains a $K_{3,4}$ subgraph. There is a unique (non-labeled) embedding of $K_{3,4}$ in the projective plane (see Figure 54). By inspection it is not possible to have another vertex adjacent to three of a, b, c, d and so $n = 0$, a contradiction.

Suppose $m = 2$ and $n \in \{2, 3, 4\}$. It follows from Euler's formula for bipartite graphs on the projective plane that $|E(G)| \leq 2|V(G)| - 2$. This implies that $n = 2$ because if $n \in \{3, 4\}$, then $|E(G)| \geq 3n + 8 > 2n + 10 = 2|V(G)| - 2$, a contradiction.

If $m = 2$ and $n = 2$, then say that v_3 is adjacent to a, b, c and v_4 is adjacent to b, c, d. Let B be the induced bipartite subgraph of F_G on partite sets $\{a, b, c, d\}$ and $\{v_1, v_2, v_3, v_4\}$. The only other edges of F_G are on vertices a, b, c, d.

Considering the six possible embeddings of the $K_{3,3}$-subgraph of B on $\{a, b, c, v_1, v_2, v_3\}$, one can see that only two of the six possible embeddings to an embedding of B and that these extensions are unique (see Figure 66). The only possible edge on $\{a, b, c, d\}$ in $E(F_G) \setminus E(B)$ is (a, d) (shown as a dashed edge in the figure). Any other edge would be in the neighborhood of cubic vertices v_3 or v_4 would violate internal 4-connectivity. Now the only possible patches on $F(G)$ are (a, d, v_1) and (a, d, v_2) and the two embedding with both of these patches are related by a single Q-Twist.

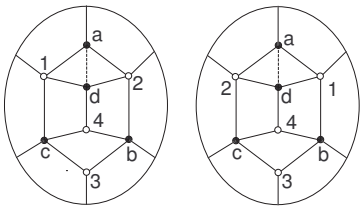

Figure 66.
Flexibility of $K_{4,4} - M_2$

Suppose $m = 1$ and $n \in \{3, 4\}$. If $n = 4$, then F_G contains a $K_{4,5} - M_4$-subgraph, which is one of the 35 minor-minimal non-projective planar graphs (see, e.g., [1]). Thus $n = 3$ and so F_G contains a $K_{4,4} - M_3$-subgraph on say partite sets $\{a, b, c, d\}$ and $\{v_1, v_2, v_3, v_4\}$ with missing edges $(v_1, b), (v_2, c), (v_3, d)$. This subgraph contains all of the edges of F_G except perhaps for any edges on $\{a, b, c, d\}$; however, adding any such edge would violate internal 4-connectivity and so this subgraph is in fact F_G itself. Since the graph is triangle free, there are no patches. Note that this graph is the alternating wheel AW_6 with rim $\{b, v_2, d, v_1, c, v_3\}$ and hubs a and v_4 whose flexibilities are described in Section 5.3.2.

Suppose $m = 0$ and $n = 4$. The subgraph of F_G minus any edges on $\{a, b, c, d\}$ is the cube and we can add all possible edge on $\{a, b, c, d\}$ and remain planar, a contradiction.

5.3.9 Frame isomorphic to the line graph of $K_{3,3}$

There are six embeddings of the line graph of $K_{3,3}$ which correspond to the embeddings of $K_{3,3}$ itself. Topologically the embeddings all look as shown in Figure 67, we show one such embedding. If F_G is isomorphic to the line graph of $K_{3,3}$, then the only patches can be as shown in Figure 67. The six possible embeddings are all related by Q-Twists as with the embeddings of $K_{3,3}$.

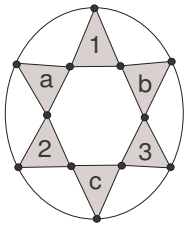

Figure 67.

6 A review of previous work

Flexibility of embeddings of graphs in the projective plane and its relationship with representativity has been studied previously in several places, e.g., [4], [5], [10], [18], and [19]. In particular, results placing an upper bound on the number of embeddings of a well-connected graph of a certain representativity have been of interest. In this section we review some of these results and provide new proofs where necessary because some errors were made in the past.

In [18, Cor.3.1] it is stated that any two distinct 3-representative embeddings of a graph in the projective plane are related by a sequence of Q-Twists, Whitney twists, and a degenerate P-Twisting operation that is there called a T-Twist. The line graph of the Petersen graph, $L(P)$, has exactly two distinct embeddings and they are not related by any of these operations. As discussed in Section 2, the two embeddings of $L(P)$ are not related by a Q-Twist. Similarly, the T-Twist operation as shown in [18, p.345] has at most seven vertices whose rotation systems change as a result of the operation. Whereas the two embeddings of the $L(P)$ have fifteen such vertices.

In [10, Thm.1.4] it is stated that any two distinct embeddings of a 3-connected graph in the projective plane are reembeddings of one of five different types. Of all of the types described, only one (which is called Type II and is shown in [10, Fig.9]) is for 3-representative embeddings. An inspection of this figure reveals that it is a full Q-Twist and the two embeddings of the Petersen graph are not related by a Q-Twist.

In our search of the previous literature, we found two results that expressly quote one or both of the two re-embedding statements in [10] and [18]; Theorem 6.1 (originally stated in [10, Thm. 5.3] and [18, Cor. 3.2]) and Theorem 6.2 (originally stated in [10, Thm. 1.3]). We provide proofs of both of these theorems based on Lemma 1.2.

Theorem 6.1 follows immediately from Lemma 1.2 but another quick proof can also be done from the work in either [19] or [2] where the minor-minimal 3-representative embeddings of graphs in the projective plane are determined.

Theorem 6.1. *If G is 3-connected and has a 4-representative embedding in the projective plane, then this embedding is the unique embedding of G in the projective plane.*

Proof. Since G is 3-connected, Lemma 1.2 implies that any flexibility of G on the projective plane is accounted for by Q-Twists and P-Twists; however, these structures all imply G has representativity at most 3, a contradiction. □

Theorem 6.2. *If $G \ncong K_6$, is 5-connected, and has a 3-representative embedding in the projective plane, then this embedding is the unique embedding of G in the projective plane.*

Proof. If we assume that G has two distinct embeddings in the projective plane, then by Lemma 1.2 the flexibilities are accounted for by Q-Twists and P-Twists. We will see that each possibility leads to a contradiction.

In a Q-Twist, any degeneracies lead to a 2-representative embedding and so the Q-Twist is non-degenerate. Now if there is any interior vertex in any one of the three quadrilateral patches, then there is a 4-separation of that vertex from one of the hinge or latch vertices, a contradiction. Thus G has 6 vertices that are the hinges and latches of the Q-Twist and since K_6 is minor-minimally 3-representative, $G \cong K_6$.

In a P-Twist or degenerate P-Twist, the patches are all triangular. Any interior vertex inside a triangular patch is separated from any vertex off of the patch by the 3 corner vertices of the patch. This is a contradiction of 5-connectivity unless all vertices of G are on this patch. In this case, G would consist of this planar triangular patch and edges outside of the patch connecting the three corners of the patch. One can check that this cannot have a 3-representative embedding, a contradiction. Thus all of the triangular patches of G contain no interior vertices and so G is a minor of the line graph of the Petersen graph, call it $L(P)$. Once we show that K_6 is the only 5-connected minor of $L(P)$, our result will follow.

We actually prove the stronger result that the only minor of $L(P)$ that is simple and with minimum degree at least 5 is K_6. If $|V(G)| = 6$, then we must have that $G \cong K_6$.

If $|V(G)| = 7$, then the only way that the minimum degree of G can be at least 5 is if G has a subgraph isomorphic to K_7 minus a 3-edge matching. This graph, however, is one of the 35 minor-minimal non-projective-planar graphs, a contradiction.

If $|V(G)| = t \geq 8$, then let $C_1, \ldots, C_t$ be the connected components of $L(P)$ that correspond to the vertices of G. Since $t \geq 8$ and $|V(L(P))| = 15$, some C_i consists of a single vertex; however, $L(P)$ is 4-regular which is a contradiction of the fact that G has minimum degree at least 5. □

In the final paragraph of [18, p.346], a third result closely related to the previous two theorems is stated. It is claimed that the number of reembeddings of a 3-connected 3-representative graph is a divisor of 12, however the reasoning is incorrect. It is stated that the number of reembeddings of a 3-connected 3-representative graph G is equal to the number of reembeddings of some minimal 3-representative minor; however this is not always the case as G may be uniquely embeddable, whereas the 15 minimal 3-representative embeddings all have non-trivial flexibilities. Here we state the theorem formally and give a complete proof. Note that the proof does not rely on Lemma 1.2, but we include this result here for completeness.

Theorem 6.3. *If G is 3-connected and has a 3-representative embedding in the projective plane, then the number of distinct embeddings of G in the projective plane is a divisor of 12. Moreover, for any divisor of 12 there is a 3-connected 3-representative graph with that number of distinct projective planar embeddings.*

Proof. Consider a connected graph G and all of its embeddings in the projective plane. These partition into equivalence classes based on equality of the underlying unlabeled embedding. Thus each equivalence class corresponds to a subgroup of the automorphism group of G. Call these equivalence classes of embeddings the *topological classes* of G.

If G has a 3-representative embedding in the projective plane, then the main result of [19] implies that the embedding has a subdivision, call it H, of one of the embeddings in [18, Fig.2]. By 3-connectivity and 3-representativity of G, the embeddings of the H-bridges of G are uniquely determined up to isotopy by the embedding of H. Thus there is an injection from topological classes of G into the topological classes of H such that the group of embeddings for a given topological class of G is a subgroup of the group of embeddings for the corresponding topological class of H. Hence the number of distinct embeddings of G in a topological class divides the number of distinct embeddings in the corresponding topological class of H.

In [19] the number of distinct embeddings of each topological class shown in [18, Fig.2] is calculated. Furthermore, note that all of the topological classes save for Classes V and VI are for different underlying graphs. Aside from H being in Classes V and VI, the number of distinct embeddings of G is a divisor of 12. For H in one of Classes V and VI, the number of distinct embeddings of G is a sum of either one or two divisors of 3, which is always a divisor of 12.

The moreover part of the statement follows from the fact that for each divisor of 12, one of the fifteen minimal 3-representative embeddings in [18, Fig.2] has that many reembeddings. □

Acknowledgement

Maharry and Slilaty would like to thank the public library of London, Ohio for their hospitality in providing a nice meeting place for them to work together.

References

[1] Dan Archdeacon, *A Kuratowski theorem for the projective plane*, J. Graph Theory **5** (1981), no. 3, 243–246.

[2] D. W. Barnette, *Generating projective plane polyhedral maps*, J. Combin. Theory Ser. B **51** (1991), no. 2, 277–291.

[3] Martin Juvan, Jože Marinček, and Bojan Mohar, *Elimination of local bridges*, Math. Slovaca **47** (1997), no. 1, 85–92, Graph theory (Donovaly, 1994).

[4] Shigeru Kitakubo and Seiya Negami, *Re-embedding structures of 5-connected projective-planar graphs*, Discrete Math. **244** (2002), no. 1-3, 211–221, Algebraic and topological methods in graph theory (Lake Bled, 1999).

[5] Serge Lawrencenko, *The variety of triangular embeddings of a graph in the projective plane*, J. Combin. Theory Ser. B **54** (1992), no. 2, 196–208.

[6] Bojan Mohar, *Uniqueness and minimality of large face-width embeddings of graphs*, Combinatorica **15** (1995), no. 4, 541–556.

[7] Bojan Mohar and Neil Robertson, *Flexibility of polyhedral embeddings of graphs in surfaces*, J. Combin. Theory Ser. B **83** (2001), no. 1, 38–57.

[8] Bojan Mohar, Neil Robertson, and Richard P. Vitray, *Planar graphs on the projective plane*, Discrete Math. **149** (1996), no. 1-3, 141–157.

[9] Bojan Mohar and Carsten Thomassen, *Graphs on surfaces*, Johns Hopkins Studies in the Mathematical Sciences, Johns Hopkins University Press, Baltimore, MD, 2001.

[10] Seiya Negami, *Re-embedding of projective-planar graphs*, J. Combin. Theory Ser. B **44** (1988), no. 3, 276–299.

[11] James G. Oxley, *Matroid theory*, Oxford Science Publications, The Clarendon Press Oxford University Press, New York, 1992.

[12] Hongxun Qin, Daniel C. Slilaty, and Xianqqian Zhou, *The regular excluded minors for signed-graphic matroids*, Combin. Probab. Comput. **18** (2009), no. 6, 953–978.

[13] Neil Robertson and Richard Vitray, *Representativity of surface embeddings*, Paths, flows, and VLSI-layout (Bonn, 1988), Algorithms Combin., vol. 9, pp. 293–328.

[14] Neil Robertson, Xiaoya Zha, and Yue Zhao, *On the flexibility of toroidal embeddings*, J. Combin. Theory Ser. B **98** (2008), no. 1, 43–61.

[15] P. D. Seymour and Robin Thomas, *Uniqueness of highly representative surface embeddings*, J. Graph Theory **23** (1996), no. 4, 337–349.

[16] Daniel C. Slilaty, *On cographic matroids and signed-graphic matroids*, Discrete Math. **301** (2005), no. 2-3, 207–217.

[17] K. Truemper, *Matroid decomposition*, Academic Press Inc., Boston, MA, 1992.

[18] R. P. Vitray, *Representativity and flexibility on the projective plane*, Graph structure theory (Seattle, WA, 1991), Contemp. Math., vol. 147, Amer. Math. Soc., Providence, RI, 1993, pp. 341–347.

[19] R.P. Vitray, *Representativity and flexibility of drawings of graphs on the projective plane*, Ph.D. thesis, The Ohio State University, 1987.

[20] Hassler Whitney, *2-Isomorphic Graphs*, Amer. J. Math. **55** (1933), no. 1-4, 245–254.

[21] Thomas Zaslavsky, *Signed graphs*, Discrete Appl. Math. **4** (1982), no. 1, 47–74.